Universidade de São Paulo

Instituto de Ciências Biomédicas

Departamento de Imunologia

Laboratório de Biologia Celular e Molecular

Dissertação de Mestrado

“Efeitos da interação Fas/FasL na diferenciação de células T CD8^{+} *in vitro*.”

Estudante de Mestrado: Marcela Bittar Araujo Lima

Orientador: Prof. Dr. João Gustavo P. Amarante-Mendes

São Paulo

2022

University of São Paulo

Institute of Biomedical Sciences

Department of Immunology

Laboratory of Molecular and Cellular Biology

Master's Degree Dissertation

"Effect of Fas/FasL interaction on $CD8^+$ T cell differentiation in vitro."

MSc Student: Marcela Bittar Araujo Lima

Supervisor: Prof. Dr. João Gustavo P. Amarante-Mendes

São Paulo

2022

Resumo

Uma abordagem científica essencial que tem sido central para o estudo da biologia e do papel das células T CD8+ durante as respostas imunes é a melhor compreensão dos mecanismos de morte/sobrevivência dessas células. Durante a fase de contração, a morte de células T antígeno-específicas pode ser alcançada por morte celular induzida por ativação (AICD) que ocorre após a ligação de Fas e FasL, ambos expressos por células T ativadas. Essa interação trimeriza o Fas, resultando no recrutamento da proteína adaptadora Fas-associated death domain (FADD) e das caspases-8 e/ou -10, criando o complexo de sinalização induzido pela morte (DISC). Então, o DISC ativa a caspase-8 ou 10 que inicia uma cascata levando à apoptose. O conhecimento e a manipulação dos mecanismos de morte/sobrevivência podem melhorar as habilidades de matar células T, otimizando as imunoterapias contra o câncer e os métodos de prevenção de infecções por vírus. Seguindo essa ideia, o projeto estudou o efeito de moléculas de morte/sobrevivência, como Fas e FasL, na ativação e diferenciação de células T CD8+ in vitro. Neste estudo, primeiro padronizamos o isolamento de células T CD8+ frescas de baços de camundongos de tipo selvagem (WT) e analisamos a ativação e diferenciação dessas células para os subconjuntos Tc0 (controle somente de ativação), Tc1 e Tc2 por Multicolor Flow Citometria (MFC) e Reação em Cadeia da Polimerase em Tempo Real (qPCR), posteriormente aplicando a mesma avaliação em camundongos deficientes em FasL (gld). Por fim, avaliamos a ativação de Tc0, Tc1 e Tc2 e a diferenciação entre camundongos WT e gld por MFC. Nossos resultados mostraram que isolamento, ativação e diferenciação eficientes em ambas as linhagens de camundongos foram alcançados. No geral, a deficiência de FasL não interfere na ativação, diferenciação e atividade efetora das células T CD8+.

Palavras-chave: *gld, mecanismos de morte/sobrevivência; marcadores de ativação, moléculas efetoras.*

Abstract

One scientific essential approach that has been central to the study of $CD8^+$ T cell biology and role during immune responses, is the better understanding of death/survival mechanisms of these cells. During the contraction phase, death of antigen-specific T cells can be achieved by *activation-induced cell death* (AICD) that occurs upon ligation of Fas and FasL, both expressed by activated T cells. This interaction trimerizes Fas, resulting in the recruitment of *Fas-associated death domain* (FADD) adaptor protein and the caspases-8 and/or -10, creating the *Death-induced signaling complex* (DISC). Then, DISC activates caspase-8 or 10 that initiate a cascade leading to apoptosis. The knowledge and manipulation of death/survival mechanisms could improve T cells killing skills, optimizing cancer immunotherapies and prevention methods of virus infections. Following this idea, the project studied the effect of death/survival molecules, such as Fas and FasL, in $CD8^+$ T cell activation and differentiation *in vitro*. In this study, we first standardized fresh $CD8^+$ T cell isolation from spleens of wild-type (WT) mice and analyzed the activation, and differentiation of these cells towards the Tc0 (activation-only control), Tc1, and Tc2 subsets by Multicolor Flow Cytometry (MFC) and Real-Time Polymerase Chain Reaction (qPCR), later applying the same evaluation on *FasL-deficient* mice (*gld*). Last, we assessed Tc0, Tc1, and Tc2 activation, and differentiation between WT and *gld* mice by MFC. Our results showed that efficient isolation, activation and differentiation in both mice lineages were achieved. Overall, FasL-deficiency does not interfere with the activation, differentiation, and effector activity of $CD8^+$ T cells.

Key Words: *gld; death/survival mechanisms; activation markers; effector molecules.*

Acknowledgments

To my **lab** and **supervisor,** who provided all material, reagents, and place for this work to happen.

To my ex-lab mates **Tandressa Bergetti** and **Mônica Rebouças**, who helped me a lot with genotyping and $CD8^+$ T cell isolation protocols and to organize the lab. Also, they taught me a lot of lab stuff (specially how to prepare solutions and cell-culture media) having extreme patience with my beginner abilities.

To my great and intelligent lab mate **Ronaldo Ribeiro**, who support me all the way from the beginning to the end of the work. He helped me with experimental design ideas, animal facility laboring, shopping materials and reagents, with equipment and protocols, cleaning work, as well as, being my only lab mate for a long period, supported me a lot psychologically.

To my dearly and big-hearted **Dra. Carolina Polonio**, who had the caring and patience to teach me everything I needed to perform the qPCR experiments with quality. Not only that, but she helped me to perform some of qPCR initial experiments, also some MFC intracellular staining experiments. She taught me the most useful lesson I will never forget, quote: “nobody makes science alone. You are allowed to get help”.

To **Prof Dr. Jean-Pierre Schatzmann Peron** and **Profa Dra. Maria Regina D’Império Lima** from *the Department of Immunology, ICB-USP*, who gave this project very important financial support.

To my most recent lab mates **Andrew Sardinha, Abolaji Olagunju** and **Samsom Kosemani,** my colleagues from *Prof. Dr. Jean-Pierre’s Lab:* **Tiago Francisco, Jonathan Zanatta, Laura Caroline de Faria** and **Sandra Muxel**); my colleague **Rogério Silva do Nascimento,** from *Profa Dra. Maria Regina’s lab*. They gave me a lot of support and tips to many routine activities.

To my dears **Joelcimar Martins da Silva** from CEFAP and **Dra. Jaqueline Polizeli Rodrigues** from DBR Biotech, who helped me perform all my MFC samples running in Cytek Nothern lights™ and BD LSR Fortessa™ equipment and taught me a lot regarding MFC technique.

To **Prof. Dr. Marcus Vinícius Chrysóstomo Baldo, Profa. Dra. Rosana Duarte Prisco, Profa. Dra. Airlane Pereira Alencar, Renato Campos Afonso** and **Bernard Lourenço Costa** from *NEPER (Núcleo de Estratégias em Planejamento Experimental e Reprodutibilidade)*. They helped me to define all best statistical analysis to this work results, also from who a learned so much regarding statistics.

To **Prof. Dr. Anderson de Sá Nunes**, **Profa. Dra. Bruna Cunha de Alencar Bargieri** and **Dra. Nágela Ghabdan**, for all the insights and tips given during my qualification exam, that deeply contributed to improve this work.

To all *ICB-USP employees*: my dear **Maria Eni do Sacramento**, who supported me so much regarding the post-graduation program issue, pointing me to all best and right directions; To my dears **Silvana Silva** and **Maria Áurea Alvarenga** who supported a lot my lab with material washing, cleaning and sterilization, making our daily work less hard.

To **ICB-USP post-graduation program**, **FAPESP** and **CNPq**, whom provided me with fellowship and financial support.

Thank you so much for everything!!

List of Figures

List of Tables

List of Abbreviations

ACAD - activated T-cell autonomous death

Actb - β-actin gene

AhR - Aryl hydrocarbon Receptor

AICD - activation-induced cell death

AP-1 - Activator protein-1

Bim - Bcl-2-like protein 11

bim$^{-/-}$ - Bim knockout mouse strain

BSA - Bovine Serum Albumin

CD62L - CD62 Ligand

CNS – Central nervous system

CTLs - cytotoxic T lymphocytes

DEPC - diethylpyrocarbonate

DISC - Death-induced signaling complex

dNTP - Deoxynucleoside triphosphate

EOMES - Eomesodermin

FADD - *Fas-associated death domain*

FasL - Fas ligand

FBS - Fetal Bovine Serum

FI-CD8 T cells – freshly-isolated CD8 T cells

GATA 3 – GATA binding protein 3

gld – generalized lymphoproliferative disease (FasL-deficient mice)

HT - heterozygous

ICB-USP - Instituto de Ciências Biomédicas, Universidade de São Paulo

IFN-γ - Interferon-γ

IL- Interleukin

IL-18R - Interleukin-18 receptor

IL-2R – Interleukin 2 receptor

IRF4 - Interferon regulatory factor 4

KLRG1 – killer-cell lectin like receptor G1

KO – *knockout*

MFC – Multicolor Flow Cytometry

MPECs – Memory precursor effector cells

NF-kB - Nuclear factor kappa-B

NFAT – Nuclear factor of activated T-cell

PAMPs - pathogen-associated molecular patterns

PBS - Phosphate-buffered saline

PCR - Polymerase Chain Reaction

PFA - paraformaldehyde

qPCR - Real-Time Polymerase Chain Reaction

ROR-γ - Retinoic acid-receptor-related orphan receptor gamma

SD – standard deviation

STAT - Signal transducer and activator of transcription

T-bet – T-Box protein expressed in T cells

T_{CM} - central memory T cells

T_{EM} - effector memory T cells

TGF-β - Transforming growth factor beta

TME - tumor microenvironment

TNF - tumor necrosis factor

T_{PM} - peripheral memory T cells

T_{RM} - resident memory T cells

WT - wild-type

Summary

1. Introduction

The Immune System protects the host against pathogens and tumors via its innate and adaptive immune responses [1]. The innate immune response comprises the first layer of protection and is composed by preexisting physical, biochemical, and microbiological barriers, as well as specialized cells that respond promptly to *pathogen-associated molecular patterns* (PAMPs). Afterwards, the adaptive immune response takes place and amplifies the mechanisms of protection. Differently from innate immune cells, B and T lymphocytes interact with pathogens using antigen-specific receptors capable of recognizing "particularities" instead of molecular patterns. Importantly, these cells are able to generate the so-called immunological memory, which is the capacity to subsequently respond faster and stronger to the same infection [2].

Effector $CD8^+$ T cells, known as *cytotoxic T lymphocytes* (CTLs), protects the body against intracellular threats, such as virus and tumors [3,4]. Cancer kills millions of people each year and is the second main cause of death worldwide, where statistics estimates that one in six deaths is cancer-related [5]. In addition, viral infections represent great danger not only individually but also to the entire human population, due to their ability to quick replicate and spread among many vertebrates, as well as their capacity to stimulate strong immune responses, bringing harmful consequences to the hosts [6]. Since the beginning of 2020, the world has been suffering from a pandemic crisis caused by a new SARS-coronavirus, known as SARS-Cov-2. This new virus is able to quick spread by human-human contact, causing respiratory disorders that may lead to death, particularly in elders and patients with co-morbidities [7–9]. In this context, CTLs play an important role as they are responsible for killing the infected cells, stopping the viruses replication, combating the infection and generating memory $CD8^+$ T. Additionally, CTLs penetrate the tumor microenvironment (TME), where they produce important immune cytokines and kill tumor cells, representing an important target for cancer immunotherapy [3].

Once naïve $CD8^+$ T cells are activated, signaling transduction cascade induced by

TCR/CD3 promotes the activation of transcriptional factors, such as *Nuclear factor of activated - cell* (NFAT), *Nuclear factor kappa-B* (*NF-kB*) and *Activator protein-1* (*AP-1*), which promote the transcription of Interleukin *(*IL)-2 and its receptor (IL-2R) and also increases the expression IL-2R α-domain (CD25) and the transmembrane C-Type lectin protein CD69 [10–15]. *NF-kB* and *AP-1* stimulates metabolic adaptation and production of effector enzymes (Perforin and granzymes), thereby transforming naïve into activated $CD8^+$ T cells [16,17]. IL-2 signaling results in massive proliferation and clonal expansion and also increases the expression of important adhesion molecules, such as CD44, a classical marker for activation and prolonged survival related to memory differentiation [18–21].

Many studies support the notion that $CD8^+$ T cells differentiate into effector subsets, such as Tc1, Tc2, Tc9, Tc17, Tc22 and Tcreg subpopulations. These subsets hold distinctive polarizing cytokines, functions, transcriptional factors (involved in subset commitment), markers and cytokines production profiles, similarly to effector $CD4^+$ T cells [17,22–26] **(Table 1).**

Tc1 cells are considered to be the conventional CTLs. They produce high levels of Interferon-γ (IFN-γ) and tumor necrosis factor (TNF)-α, and low levels of IL-4 [27–29]. Probably because of their high expression of cytolytic molecules, such as Granzyme B and Perforin, they present superior cytotoxic activity [30,31]. When naïve cells are activated, the presence of IL-12 triggers a signaling cascade that increases expression of the transcription factors *Signal transducer and activator of transcription (STAT) 4*, *T-Box protein* expressed in T cells *(T-bet)* and *Eomesodermin* (*EOMES*), which together shape the commitment to the Tc1 pathway [32,33]. In addition, the high expression of Interleukin-18 receptor (IL-18R) has been shown to be a particular characteristic of the Tc1 lineage [26,34]. Tc1 cells seems to be important to fight viral infections [35,36] and tumors [31,37], but some recent studies have been demonstrated that Tc1 is also associated to chronic inflammation mechanisms in some small intestine autoimmune disorders, such as Inflammatory Bowel Disease [38–40] .

Table 1: Characterization of effector CD8⁺ T cells subsets by cytokines and transcriptional factors involved in their polarization, main known surface markers, production of cytokines and effector molecules, described function and cytotoxicity capacity.

Subset	Polarization Cytokines	Transcriptional factors	Effector Cytokines and Molecules	Function	Cytotoxic Activity
Tc1	IL-12	T-bet, Eomes, STAT4	IFN-γ^{high} , TNF-α^{high}, Granzyme B^{high}, Perforin^{high} (IL-4, IL-5, IL-13) $^{low/-}$	Cytotoxic Killer (CTLs). Viral infections clearance and critical antitumor activity Associated with gut autoimmune disorders	Yes
Tc2	IL-4	GATA3, STAT6	IL-4^{high}, IL-5^{high}, IL-13^{high}, IFN-$\gamma^{low/-}$	Direct linked to allergy phatogenesis	Yes/No (Controversy)
Tc9	IL-4, TGF-β	IRF4, STAT6	IL-9, IFN-$\gamma^{low/-}$	Very unclear. Association with pro/anti inflammatory activities and important anti-tumor action.	No
Tc17	IL-6, TGF-β	RORγT, IRF4, STAT3	IL-17^{high}, IL-21^{high}, IL-22^{high} (IFN-γ, Granzyme B)$^{low/-}$	Associated with the TME, chronic inflammation and autoimmune disorders. Protection against fungal infection.	No
Tc22	IL-6, TNF-α, AhR agonist	AhR	IL-22, TNF-α, IL-2 (other lineages' cytokines) $^{low/-}$	Very unclear. Great antitumor activity in some studies.	Yes

Like effector CD4⁺ subsets well stablished features, the cytokines IFN-γ, IL-4, IL-9, IL-17 and IL-22, also the transcription factors, *T-bet, GATA3, IRF4, RORγT* and *AhR* can also be decisive to distinct and identify each effector CD8⁺ subset [24,26,38]. (Figure retrieved and adapted from St. Paul, M & Ohashi, P., 2020).

Tc2 differentiation is stimulated by IL-4, which activates a cascade via *STAT6* and *GATA binding protein 3* (*GATA3*). Tc2 produces very low level of IFN-γ and seems to display a weak cytotoxic ability[26,41–44]. Similarly to Th2, Tc2 is characterized by increased production of IL-4, IL-5 and IL-13, and the ability to stimulate IgE production and eosinophils recruitment to the respiratory tract, having an important role in allergy development [44–48].

Tc9 is a relatively new subset that is not yet completely accepted in the literature. However, studies have described it as a subset involved in pro-inflammatory activity related to small intestine and respiratory tract. In addition, adoptive transfer studies suggested that Tc9 cells may have important antitumor activity [49–52]. Their polarization is also driven by IL-4 in addition to *Transforming growth factor beta* (TGF-β), which induces *Interferon Regulatory factor 4* (*IRF4*) and *STAT6* signaling driving the transcription of genes related to this lineage. They produce IL-9 as a signature cytokine, but also IL-10. Similarly to Tc2 cells, Tc9 cells are poorly cytotoxic and IFN-γ producers [51,53–56].

The relationship among Th1/Tc1 and Th2/Tc2 is also reflected at the level of Th17/Tc17. Tc17 cells are polarized by IL-6 in combination with TGF-β, which triggers the activation of the transcriptional factors *Retinoic Acid-Receptor-Related Orphan Receptor gamma* (*ROR-γ)t* , *IRF4* and *STAT3* that, in combination, promotes transcription of genes associated with Tc17 lineage commitment. They produce high levels of IL-17, IL-21 and IL-22, but low levels of IFN-γ and granzyme B, and have no considerable cytotoxic activity [29,57–61]. Although the biological role of these cells still unclear, few studies have shown a particular function of Tc17 on the clearance of fungal and other infections. Besides, other studies have revealed a contribution of Tc17 cells to increase chronic inflammation and to suppress immune responses in the TME of many tissue-specific cancers, and particularly skin and small intestine autoimmune diseases and allogenic transplantation [21,38,40,56–58,62–66].

The last and the more recently described subset, Tc22, have been demonstrated to have good cytotoxic capacity probably due to its abundant production of granzyme B. In addition, it has been reported that Tc22 subset has important antitumor activity and it is protective against viral infections [67]. In addition, Tc22 has significant participation in immune response during transplantation complications [68], even though its biological role remains obscure. After activation, the presence of IL-6 and TNF-α, in combination with an agonist of the *Aryl hydrocarbon Receptor*

(*AhR*), activates a cascade mediated particularly by the transcriptional factor *AhR*, endorsing the Tc22 subset differentiation and consequently the production of IL-22, TNF-α and IL-2 [24,26,34,69,70]. Importantly, although the mechanisms of $CD4^+$ T cells differentiation are well established, the molecular machinery responsible for effector $CD8^+$ T cells differentiation into diverse cellular phenotypes remains unclear [22,71,72].

When the threat is finally contained or $CD8^+$ T cells are being chronically activated, mechanisms of programmed cell death secure the elimination of unnecessary or potentially harmful antigen-specific effector $CD8^+$ T cells [73]. During this contraction phase, death of antigen-specific T cells can be achieved by two different processes: *activation-induced cell death* (AICD) and *activated T-cell autonomous death* (ACAD), both involving the well-described extrinsic and intrinsic apoptosis pathways (**Figure 1**) [73,74].

AICD occurs through Fas-*Fas ligand* (FasL) interaction, in which Fas is the prototype of the death receptor family, commonly expressed by many cell types, particularly activated T cells. Upon ligation, FasL also expressed by activated T cells, trimerizes Fas, resulting in the recruitment of *Fas-associated death domain* (FADD) adaptor protein and the caspases-8 and/or -10, creating the *Death-induced signaling complex* (DISC). Caspase-8 or 10 are activated and initiate a cascade leading to apoptosis. In contrast, ACAD occurs via *Bcl-2-like protein 11* (Bim), a BH3 domain-only member of Bcl-2 family. Bim can be activated by multiple stress signals, including oncogene activity, chemotherapeutic drugs, and absence of extracellular survival/activation signals [75]. Upon activation, Bim antagonizes two anti-apoptotic proteins of the Bcl-2 family (Bcl-2 itself and Bcl-xl) that are constantly inhibiting the major pro-apoptotic proteins from the same family (Bax and Bak), thereby maintaining mitochondrial membrane stability. Once Bax and Bak are free from Bcl-2 or Bcl-xl restraint, Bax-Bak oligomerizes and creates pores on the mitochondrial outer membrane. Because of that, mitochondrial intermembrane content, primarily cytochrome c, overflow to the cytosol binds to APAF-1 and activates caspase-9, initiating

apoptosis [76,77]. While AICD is dependent on the TCR restimulation, ACAD is initiated by the absence of external stimuli (antigen) [73,74].

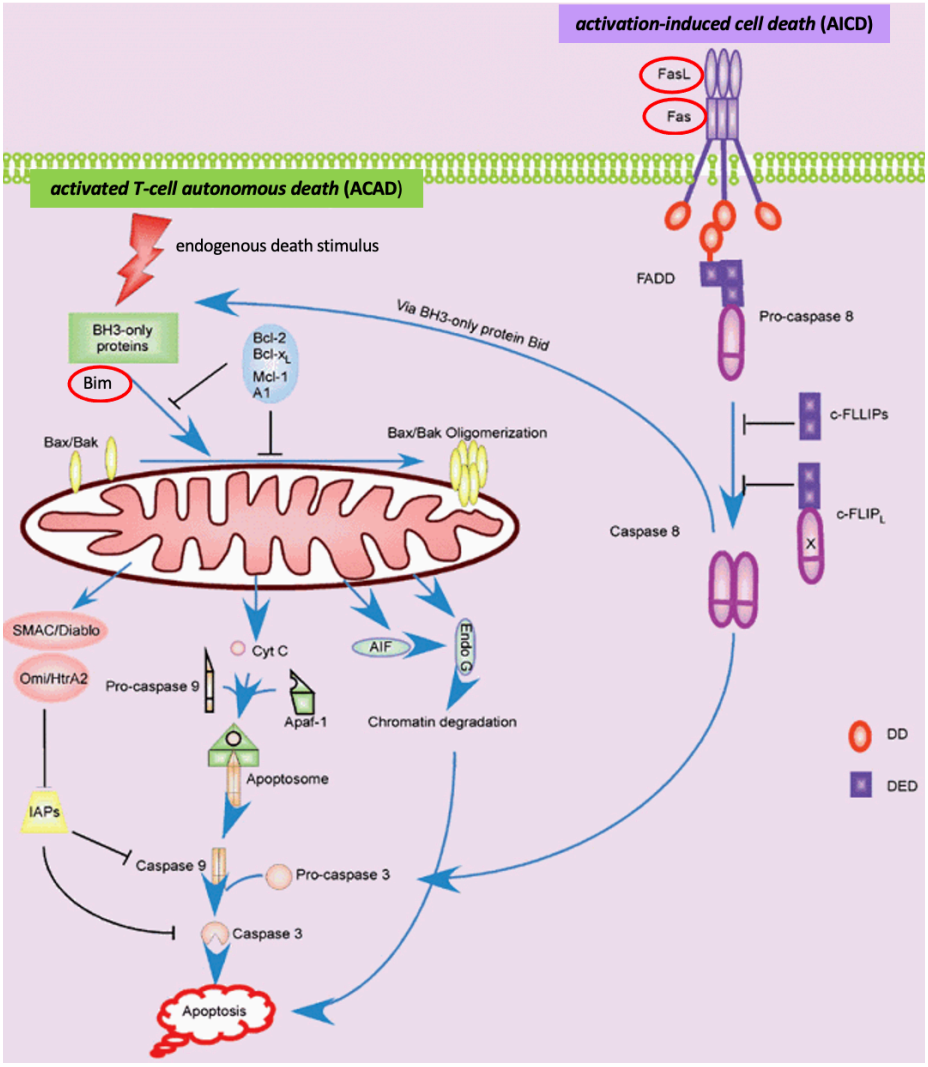

Figure 1: Antigen-specific T cell death mechanisms. Fas-FasL interaction leads to trimerizaton of Fas, in which FADD adaptor protein binds to other death effector domain proteins in Fas cytoplasmic area, generating DISC complex. DISC eventually activates a cascade of effector caspases through caspase- 8 or 10, resulting in apoptosis (AICD). As the result of a drop of antigen stimulation, Bim protein gets activated and breaks the blocking effect of anti-apoptotic Bcl-2 and Bcl-xl on both Bax and Bak proteins, thereby inducing their oligomerization and mitochondrial outer membrane pore (MOMP) formation. As a consequence, cytochrome c and other proteins leak to the cytosol activating the effector caspases that leads to apoptosis (ACAD)[78].(Figure retrieved and adapted from Zhang N.,et all, 2005).

Most importantly, these cell death mechanisms are essential part of the immune regulation, as they maintain lymphocyte homeostasis, prevent exacerbated inflammation, and contribute to tolerance [79]. Although the manipulation of these survival mechanisms could improve the amplitude of $CD8^+$ T cell responses, the effect of signaling pathways emanating from Fas/FasL interaction and/or dependent on the expression of Bim to the differentiation of $CD8^+$ T cell subsets and their effector capacity remains obscure [4,80]. In addition, it is not clear how Bim activation and Fas/FasL interaction shape the memory cell repertoire/compartment. After contraction phase, the remaining $CD8^+$ T cells differentiate into *central memory T cells* (T_{CM}), located in the secondary lymphoid organs, *effector memory T cells* (T_{EM}) that circulates or populates the tissues [22,81], and *resident memory T cells* (T_{RM}), which does not circulates and rather populates tissues permanently [81–84]. More recently, some studies also identified a new subpopulation described as *peripheral memory T cells* (T_{PM}) based on the expression of the fractalkine receptor (Cx3Cr1), during chronical infections[85,86]. These subpopulations (long term cells) create a heterogeneous pool of memory cells that can fluctuate depending on the antigen and duration of exposure. Also, they basically have the potential to effectively produce a second pool of functional terminal-effector cells, providing immune-surveillance adapted to quickly and carefully respond to a re-infection [22,23,81].

In fact, $CD8^+$ T cell differentiation into effector and memory subsets during antigen exposures have been explained by two different models [87]. The first model claims that once activated, naïve $CD8^+$ T cell differentiates into effector subsets and during contraction phase, each subset individually develops memory precursors [88,89]. The cytotoxic activity of these memory precursors and their high expression of effector molecules such as granzyme B support the notion that these cells have previously passed through an effector stage [90]. In contrast, the second model proposes that once naïve cells are activated (in its early activation stage), memory precursors,

named as *memory precursors effector cells* (MPECs), are originated and following stimuli, those precursors could later differentiate into memory subsets and short-lived effector subsets [91,92].

The distinct memory subpopulations follow the same rule as the effector subsets and can be characterized by the expression levels of surface markers, transcriptional factors, cytokines production, also function and location **(Table 2)**. The expression of CD127, CD27, CCR7, CD44, *CD62 Ligand* (CD62L) and Cx3Cr1 also the transcriptional factors *T-bet, TCF1, Blimp1* and *Hobit* could also identify the distinct memory subpopulations. T_{CM} cells show increased expression of CD62 Ligand (CD62L), CD127, CD27, CD44 and CCR7, but low expression of KLRG1 and Cx3Cr1, has an elevated proliferation ability and decreased cytotoxic activity explained by these population been substantially located in lymph nodes [21,55,64,65,84,93].

Table 2: Characterization of the memory $CD8^+$ T cells subpopulations in mice by phenotype markers, function, location/trafficking and respective transcriptional factors expressed.

Subpopulation	Surface Markers	Trancscription Factors	Location	Function
T effector memory (T_{EM})	$KLRG1^{high}$, $CD44^+$, $CCR7^{low}$, $CD62L^{low}$ $Cx3Cr1^{high}$, $CD27^{low}$, $CD127^{high}$	$T\text{-}bet^{high}$, $Blimp1^{high}$, $STAT4^{high}$ $ID2^{high}$	Circulation	↑ Cytotoxicity ↓ Proliferation
T central memory (T_{CM})	$KLRG1^{low}$, $CD44^{high}$, $CCR7^{high}$, $CD62L^{high}$ $Cx3Cr1^{low}$, $CD27^{high}$, $CD127^{high}$	$T\text{-}bet^{low}$, $Eomes^{High}$, $TCF1^{high}$ $Bcl6^{high}$, $STAT3^{high}$, $ID3^{high}$	Secondary Lymphoid organs	↓ Cytotoxicity ↑ Proliferation
T resident memory (T_{RM})	$CD69^{high}$, $CD103^{high}$, $CD49a^{high}$ $KLRG1^{low/-}$, $CCR7^{low}$, $CD62L^{low}$ $Cx3Cr1^{low/intermidiate}$, $CD127^{high}$	$T\text{-}bet^{low}$, $Blimp1^{high}$, $Hobit^{High}$ $Eomes^{-/low}$, $TCF1^{low}$	Tissue resident	Tissue alert Proliferation +/-

The distinct expression levels of surface markers such as KLRG1, CD127, CCR7, CD27, CD44 and CD62L and transcription factors T-bet, TCF1, Blimp1 and Hobit are fundamental to characterize the three memory subpopulations. In addition, proliferation and toxicity capacities, also location of the cells, are different among memory subpopulations and could help identify and characterize each one of them [21,55,64,65,81,84,93].

In contrast, T_{EM} cells express high KLRG1, Cx3Cr1, also CD127 and CD44, but low CD62L, CD27 and CCR7. They are poorly proliferative but they show high cytotoxicity, also explained by its capacity to circulate through the whole body and be ready to act upon any threat encounter [21,55,64,86,92,93]. T_{RM} cells show similar levels of some important surface markers of T_{EM} ($CD62L^{low}$, $CCR7^{low,}$) and T_{CM} ($KLRG1^{low}$, $CD127^{high}$, $T\text{-}bet^{low}$). On the other hand, they exclusively express high levels of transcriptional factor *Hobit*, and surface markers CD69, CD103 and CD49 [65,93,94]. They are located strictly in tissues and have a basic function of local immunosurveillance and quickly alert the tissue by any threat re-encounter [95,96]. The recent described T_{PM} cells express unique intermediate levels Cx3Cr1 and other markers, also cytotoxicity and proliferation. They basically are a subpopulation that show better stability and self-renewal capability, also can migrate to peripheral tissues [86,97]. However, this differentiation process and the physiological importance of those subpopulations is still yet in development.

2. Objectives

Main Objective

The objective of this work was to investigate the role of pro-apoptotic molecules, such as Bim and FasL, on *in vitro* $CD8^+$ T cell differentiation to the known effector subpopulations.

Specific Goals

- To optimize experimental conditions for *in vitro* $CD8^+$ T cell isolation, in C57BL6 WT mice.
- To optimize experimental conditions for *in vitro* $CD8^+$ T cell activation to Tc0 (non-polarized condition), in C57BL6 WT mice.
- To optimize experimental conditions for *in vitro* $CD8^+$ T cell differentiation to Tc0 (non-polarized condition), Tc1 and Tc2 effector subsets, in C57BL6 WT mice.

- To compare the activation and differentiation profile of Tc0, Tc1 and Tc2 subsets in WT, and *gld* animals.

3. Materials and Methods

Animals

C57BL/6 WT and *gld* mice, between 6 and 8 weeks of age, male or female were obtained from the animal facility of the Institute of Biomedical Sciences, University of São Paulo (ICB-USP) and maintained under institutional guidelines conditions. Animals were kept in ventilated racks under controlled conditions of temperature, humidity and lighting (12-hour light/dark cycle). All manipulation were subject to approval by the Animal Manipulation Ethics Committee of the ICB-USP before any experimental procedure, abiding by the international laws of animal ethics.

Extraction of splenocytes and isolation of $CD8^+$ T cells

WT and *gld* mice were euthanized by inhalation of isoflurane solution (BioChimico®) followed by cervical dislocation. Spleens were removed and placed into 6-well tissue culture plates or Petri dishes containing RPMI-1640 supplemented with 10% *fetal bovine serum* (FBS). Then, spleens were squeezed by a 0.45mm x 13mm syringe plunger to release splenocytes into the plate solution. Cell suspension was filtered in a 70 μm cell strainer to remove tissue debris and transferred to 50 mL falcon tubes. Next, splenocyte suspensions were centrifuged at 350g for 10 min at 4°C. Supernatants were carefully discarded and pellets were mixed and resuspended in 2ml/spleen of hypotonic solution buffer (*0.15 mM NH4Cl, 1 mM KHCO3, 0.1 mM Na EDTA, pH 7.2–7.3*) for 2 minutes to lyse red blood cells. Then, samples were washed with MACS Buffer (*Phosphate-buffered saline (PBS) 1X, 5% of Bovine Serum Albumin (BSA), 0,4% of 0,5mM EDTA, pH 8.0*), centrifuged again and resuspended with the same buffer. Cell concentration and viability were evaluated by 0.2% trypan blue staining in a Neubauer

hemacytometer and Nikon Microscope or in an Automated Cell Counter (*Countess II FL cell counter, Life Technologies™*). After that, $CD8^+$ T cells were negatively selected from samples containing 5 x 10^7 - 1 x 10^8 splenocytes using the *EasySep™ Mouse $CD8^+$ T Cell Isolation Kit (StemCell™ Technologies)*, following manufacturer instructions. Briefly, pools of spleen cells were mixed with a variety of lineage-specific antibodies, which does not include $CD8^+$ T cells one, then separated by a magnet (*EasySep™ Magnet – StemCell™ Technologies),* and eliminated from samples. Freshly-isolated $CD8^+$ T cell (FI- CD8 T cells) concentration and viability were evaluated following same procedure.

In vitro subset Activation and Differentiation

For generation of effector $CD8^+$ T cell subsets - Tc0, Tc1 and Tc2 - FI-CD8 T cells (in proportion of 2 x 10^5 cells/ well) were first separated in 1,5 ml sterilized tubes and centrifuged at 350g for 10 min at 4°C. Afterwards, cells were resuspended with supplemented medium (RPMI-1640, 10% FBS, 1% Non-essential Amino Acids – NEAAs, 1% sodium pyruvate, 1% penicillin/streptomycin, 1% vitamins, 1% L-glutamine 1% β-Mercaptoethanol) containing anti-CD3/CD28 antibodies coupled with magnetic beads (*Dynabeads™ Mouse T-Activator CD3/CD28 for T-Cell Expansion and Activation – Gibco™*) in proportion of 5μL / 1 x 10^6 FI-CD8 T cells and incubated at 37°C for 45 min-1h. In parallel, another Mix for each subset were prepared containing same supplemented medium, 20 ng/mL (or 30 U/mL) of IL-2 (diluted with PBS 1x from the *IL-2 human stock at 10^5 U/ml, Sigma-Aldrich®)* and specific polarizing cytokines: 5 ng/mL of IL-12 (diluted with PBS 1x from the *IL-12 mouse stock at 200μg /mL*, BD Pharmingen™) for Tc1; 20 ng/mL of IL-4 (diluted with PBS 1x from the *IL-4 mouse stock at 200μL /mL*, BD Pharmingen™*)* + 2,5μg/mL of anti-IFN-γ mAbs (stock at 2,5 mg/ml, *Biolegend®)* for Tc2 [69]. Each subset Mix were distributed in the 24-well flat-bottomed plates in volume of 800μL/well. Last, the samples were

distributed in the same plates in volume of 200μL/well and placed for culture under 5% CO_2 at 37°C for 3 or 5 days.

Post-culture Treatment

After activation and differentiation, anti-CD3/CD28 antibodies coupled to magnetic beads were eliminated from the cultures using the magnet column. Samples containing Tc0, Tc1 and Tc2 were washed and either resuspended in RNA-isolation solution (*Trizol™ reagent, Invitrogen*) and kept in -80°C freezer for minimum 48h for qPCR protocol or used immediately for Extracellular and Intracellular staining and flow cytometry.

Real-Time Polymerase Chain Reaction (qPCR) analysis

1.1.1. RNA extraction

$CD8^+$ T subset samples previously stored in *Trizol* were submitted to RNA isolation from DNA and proteins. The upper transparent portion of samples, which contains RNA, were cautiously removed, avoiding contamination, transferred to another tube where 500μL of isopropanol were added and then kept at room temperature for 10 minutes. Samples were centrifuged at 12000g for 10 minutes and the supernatants were discarded. Pellets were washed three times in 1 mL of 75% ethanol and centrifuged at 7600g for 5 minutes at 4°C. Ethanol was removed, tubes were kept inverted on the bench at room temperature until the pellet was completely dry out, and then resuspended again in 25μL of sterilized *diethylpyrocarbonate* (DEPC) water at 0.1%. Purified total RNA was quantified using *NanoDrop™ 2000/2000c Spectrophotometer (Thermofisher Scientifics)*, and concentration provided as ng/μL.

1.1.2. cDNA synthesis

For the synthesis of cDNA, 2 μg of mRNA (previously extracted) were diluted in DEPC water to reach 14.2μL. Then, 5.8μL of a master mix containing 0.8μL of dNTPs, 2μL of RT random primers, 2μL of RT Buffer, and 1μL of multiscribe reverse transcriptase enzyme were added. Samples were subject to cycles of 10 minutes at 25°C; 2 hours at 37°C; and 5 minutes at 85°C) in a thermocycler (*QuantStudio™ 3 Real-Time PCR System, 96-well, 0.2 mL, laptop – Applied Biosystems™*). After that, 180μL of DEPC water were added to each sample containing now cDNA, which were finally kept at -20°C.

1.1.3. Quantification of messenger RNA (mRNA) expression

To analyze the expression of transcriptional factors (*T-bet* and *Gata-3*) and effector molecules (IFN-γ, IL-4 and IL-18R) involved in CD8 T cell differentiation, the obtained cDNA samples were submitted to a quantitative PCR reaction. For each reaction, 4.6μL of cDNA sample were added to a mix containing 5.0μL of *SYBR Green Master Mix (Applied Biosystems™)* and 0.4 μL of Custom Primers' oligo sequences (*Invitrogen™*) for transcriptional factors and effector molecules genes: *Tbx21* (forward: 5'-AGCAAGGACGGCGAATGTT-3'; reverse: 5'-AGTAGGCCACATTACACTGCT-3'); *Gata3* (forward: 5'- CTCGGCCATTCGTACATGGAA-3'; reverse: 5'-GGATACCTCTGCACCGTAGC-3'); *Ifng* (forward: 5'-ATGAACGCTACACACTGCATC-3'; reverse: 5'- CCATCCTTTTGCCAGTTCCTC-3'); *Il4* (forward: 5'-GGTCTCAACCCCCAGCTAGT-3'; reverse: 5'-GCCGATGATCTCTCTCAAGTGAT-3'); *Il18r* (forward: 5'-ACTTTTGCTGTGGAGACGTTAC-3'; reverse: 5'-CCGGCTTTTCTCTATCAGTGAAT-3'); *Actb* (forward: 5'-GGCTGTATTCCCCTCCATCG-3'; reverse: 5'-CCAGTTGGTAACAATGCCATGT-3'). The PCR samples were taken again to the thermocycler (*QuantStudio™ 3 Real-Time PCR System, 96-well, 0.2 mL, laptop – Applied Biosystems™)* for a cycle of 40 repeats for the following stages: 2 minutes at 50°C; 2 minutes at 95°C; 95°C for seconds and 1 minute at 60°C).

All control curves provided by real time cycling were normalized by the expression of *Actb*. Each specific gene expression was obtained by ΔCT, which is the *CT* (*Cycle threshold*) of the target gene subtracted of the *CT* of the constitutive gene. The relative gene expression among subsets was represented by *fold change,* calculated by the respective formula:

$\mathbf{2}^{(-\frac{Fold}{\Delta\Delta CT})}$, where $\frac{Fold}{\Delta\Delta CT}$ = ΔCT *(sample)* $-\Delta CT_{mean}$ *(calibrator).*

The *calibrator* was the control subset (Tc0), and ΔCT_{mean} was obtained from the mean of four replicates of Tc0 ΔCT. Each *sample* was equivalent to a replicate.

Multicolor Flow Cytometry (MFC)

1.1.4. Extracellular staining

For the analysis of surface activation and effector/memory markers, 1 x 10^6 splenocytes, FI-CD8 T cells, Tc0, Tc1 and Tc2 were stained with the following conjugated antibodies: CD8a (BV510 and BB515, clone *53-6.7, BD Horizon™*); CD4 (PE, clone *H129.19, BD Pharmingen™*); CD69 (BV480, clone *H1.2F3, BD Pharmingen™ and BD OptiBuild™ ;* FITC*,* clone XMG1.2, *eBioscience™*), CD25 (APC, clone *PC61.5, eBioscience™*), CD44 (PE, clone *IM7, eBioscience™*), KLRG1 (BV786, clone *2F1, BD Horizon™*) and CD62L (PE-CF594, clone *MEL-14, Biolegend®*); as well as the viability dye *LIVE/DEAD™ Fixable Near-IR Dead Cell Stain Kit, Invitrogen™*). Dilution for all antibodies varies between 1:100 and 1:1000 in MACS Buffer and was previously optimized for our flow cytometers and experimental conditions. Samples were stained at 4°C for 30 min, then washed with 1 mL of MACS Buffer, and fixed with 300μL of paraformaldehyde (PFA) 1%. Unstained samples (US) of each cell population were used as negative controls.

1.1.5. Intracellular staining

For the analysis of effector molecules, 1 x 10^6 FI-CD8 T cells, Tc0, Tc1 or Tc2 were treated with Brefeldin-A (*Biolegend®*) under 5% CO_2, at 37°C for 4h. Then, samples were stained with a mix of the following conjugated antibodies: CD8a (BB515, clone *53-6.7, BD Horizon™*), FasL/CD178 (PE, *MFL3, eBioscence™*) and *LIVE/DEAD™ Fixable Near-IR Dead Cell Stain, followed by* IFN-γ (PE-CF594, clone *XMG1.2, BD Horizon™*), TNF-α (BV650, clone *MP6-XT22, BD Horizon™*), Granzyme B (PE-Cy7, clone *NGZB, eBioscence™*), Perforin (APC and PE, clone *eBioMAK-D, eBioscence™*), IL-4 (BV711, clone *11b11*, *BD Horizon™),* using intracellular staining kit (*FoxP3 Staining Buffer Set, eBioscence™*) following manufacturer's instructions. An unstained sample (US) of each cell population were used as negative control.

1.1.6. Multicolor Flow cytometry (MFC) and data analysis.

All samples were run in *Cytek Nothern lights™* or *BD LSR Fortessa™ Cell Analyzer* using *BD FACSDiva™ Software*. For each stained Tc0 samples of 5 days-culture, 3 x 10^5 events were recorded. For the rest of all stained samples and for negative control samples, 5 x 10^5 and 5 x 10^4 events were record, respectively. Each staining panel (extracellular and intracellular) was compensated using compensation beads (*BD™ CompBeads Anti-Mouse Ig, κ/Negative Control Compensation Particles Set, BD Biosciences*) or Tc0 samples, stained with each antibody individually. Negative controls used were either unstained compensation beads or Tc0 samples.

All data were analyzed by *BD FlowJo™ V.10* software using the same gate strategy (**Figure 2**). Doublets, cellular debris and dead cells were successively excluded using FSC-H x FSC-A, SSC-A x FSC-A and SSC-A x Live/Dead staining analysis, respectively. Remaining data were provided as frequency of $CD8^+$ live events. All gates were defined based on their respective non-stained negative control.

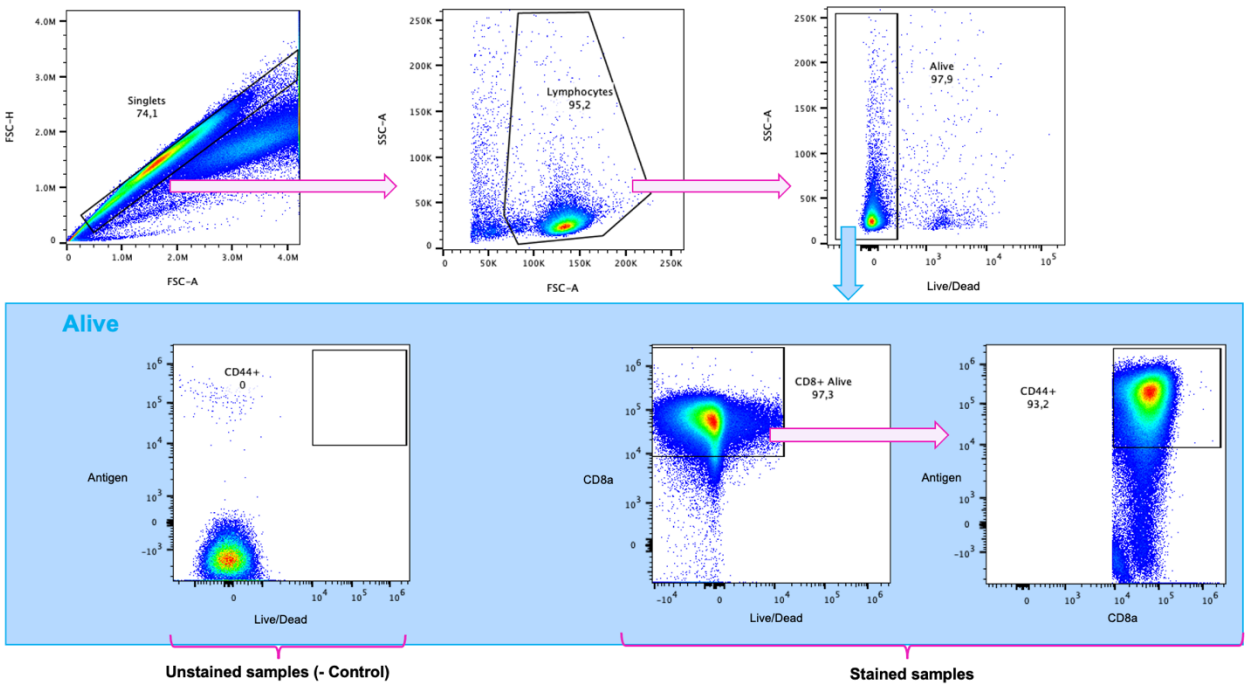

Figure 2: BD FlowJo™ gate strategy for the analysis of CD8⁺ T cells. All samples were first gated for singlets, following by lymphocytes and live cells. For negative control samples, all gates for the antigens of interest are selected inside the live cells' gate, while for stained samples, the antigens are designated inside viable CD8a gate.

Statistical Analysis

All $CD8^+$ T cell activation and differentiation experiments by MFC were performed in triplicates, 1 to 3 times independently. Statistical analysis of MFC was based on the Frequency and Mean Fluorescence Intensity (MFI) of live $CD8^+$ T cells expressing activation markers and effector molecules. Frequency was considered as a relative percentage given by the total number of viable $CD8^+$ events, also positive for each specific molecule, compared to the total number of live events. In addition, qPCR experiments were performed in quadruplicates in 2 independent experiments and analyzed as described above. Since this presented work was completely exploratory, statistical significance of frequency, MFI and fold change was assumed as $\alpha < 0.05$. All data was analyzed in *Graphpad Prism 9* software using the following strategies.

1.1.7. WT Comparison of FI-CD8 T cells, Tc0 from 3 and 5 days-culture by MFC.

Frequency and MFI values of a single experiment per population performed individually were analyzed by a single factor (subset) per each dependent variable (activation markers) using ordinary one-way ANOVA. Multiple comparisons were corrected by Tukey's test. Statistical sample size (N) was 3 (3 animals for FI-CD8 T cells and 3 culture wells for Tc0 of both distinct time-cultures).

1.1.8. WT x gld analysis of FI-CD8 T cell activation markers by MFC.

Frequency and MFI values of a single experiment were analyzed by a single factor (lineage) per each variable (activation markers) using unpaired two-tailed Welch's t-test. Significance was assumed as $\alpha < 0.008$, due to Bonferroni's correction of multiple comparisons. N was 3 (3 animals per lineage).

1.1.9. qPCR analysis

Fold change values of one experiment were analyzed by a single factor (subset) per each dependent variable (transcription factors and cytokines) using ordinary one-way ANOVA. Multiple comparisons were corrected by Tukey's test. N was 4 (4 culture wells for each subset).

1.1.10. WT x gld: Tc0, Tc1 and Tc2 analysis of activation markers by MFC.

Frequency and MFI values of three independent experiments were analyzed by 2 factors (subset and lineage) per each dependent variable (activation markers) using ordinary two-way ANOVA, confirming normality. Multiple comparisons were corrected by Tukey's or Šídák's tests. N = 9 (3 culture wells for each subset per test).

1.1.11. WT x gld: Tc0, Tc1 and Tc2 analysis of effector molecules by MFC.

Frequency and MFI values of two independent experiments were analyzed by 2 factors (subset and lineage) per each dependent variable (effector molecules) using ordinary two-way

ANOVA, confirming normality. Multiple comparisons were corrected by Tukey's or Šídák's tests. N = 9 (3 culture wells for each subset per test).

4. Results

Isolation of splenic $CD8^+$ T cells

We started our project optimizing the efficiency of $CD8^+$ T cell isolation using negative selection protocol. To achieve that, we performed a great number of independent experiments using spleens from male and female WT animals, aged between 6-8 weeks and reagents obtained from different suppliers. Total splenocytes and freshly isolated $CD8^+$ T (FI-CD8 T) cells were stained for viability, CD8a, and CD4 and analyzed by flow cytometry (**Figure 3**). Regarding viability, all splenocytes and FI-CD8 T cell samples maintained similar and high frequency of live cells (**Figure 3**). Furthermore, all splenocyte samples demonstrated comparable frequency of $CD4^+$ (around 15%) and $CD8^+$ (around 10%) T cells, expected from healthy animals (**Figure 3**). After numerous tests, we were able to obtain a high and constant amount of purified FI-CD8 T cells (80-90%), with no contamination of $CD4^+$ cells (**Figure 3**).

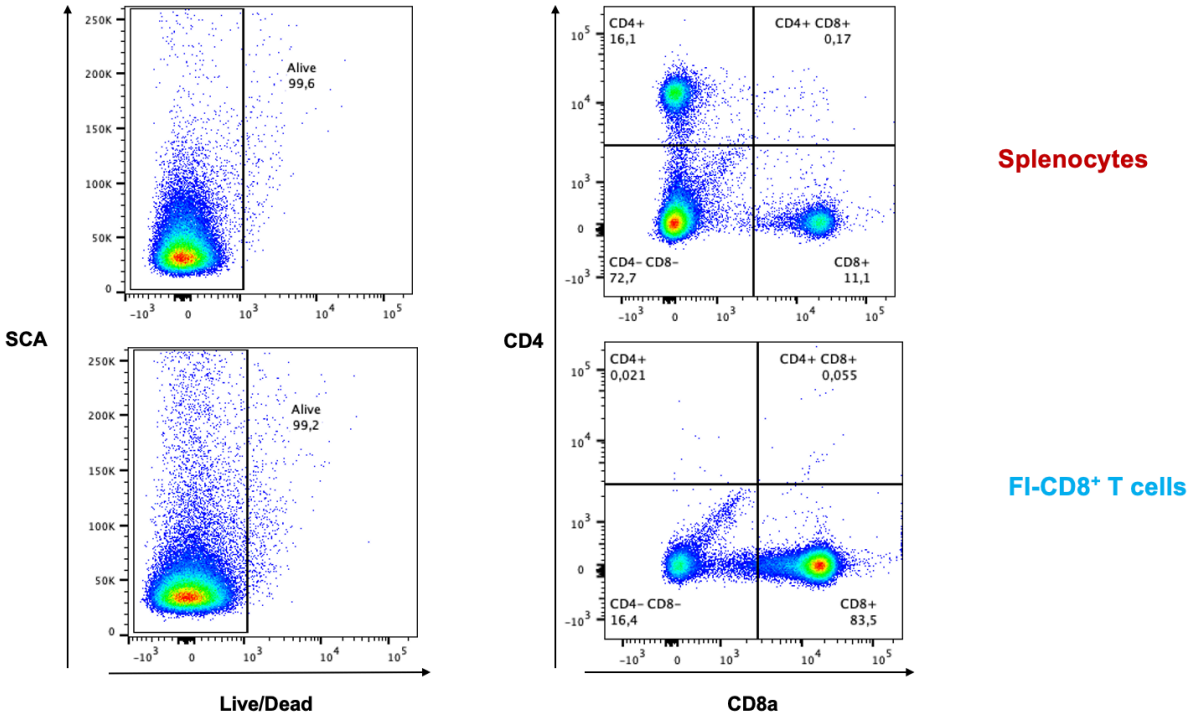

Figure 3: Isolation of fresh CD8⁺ T cells using Negative Selection Kit. Flow cytometry plots showing viability and isolation efficiency of splenocytes and freshly-isolated CD8 T cells (FI-CD8 T cells) samples from WT animals using StemCell™ Technologies kit. The presence of $CD4^+$ cells are also demonstrated in the two samples.

In vitro activation of CD8⁺ T cells

Once the isolation protocol was finally optimized and validated, we established the best condition of *in vitro* CD8 T cell activation. We compared data from three independent experiments where we cultured 2 x 10^5 FI-CD8 T cells/well of 24-well flat-bottom plates containing IL-2 and anti-CD3/anti-CD28 magnetic beads, for 3 and 5 days to generate Tc0. Samples were stained for selected activation markers, such as CD25, CD69, CD44, KLRG1 and CD62L, using the extracellular staining protocol and then analyzed by MFC (**Figure 4**).

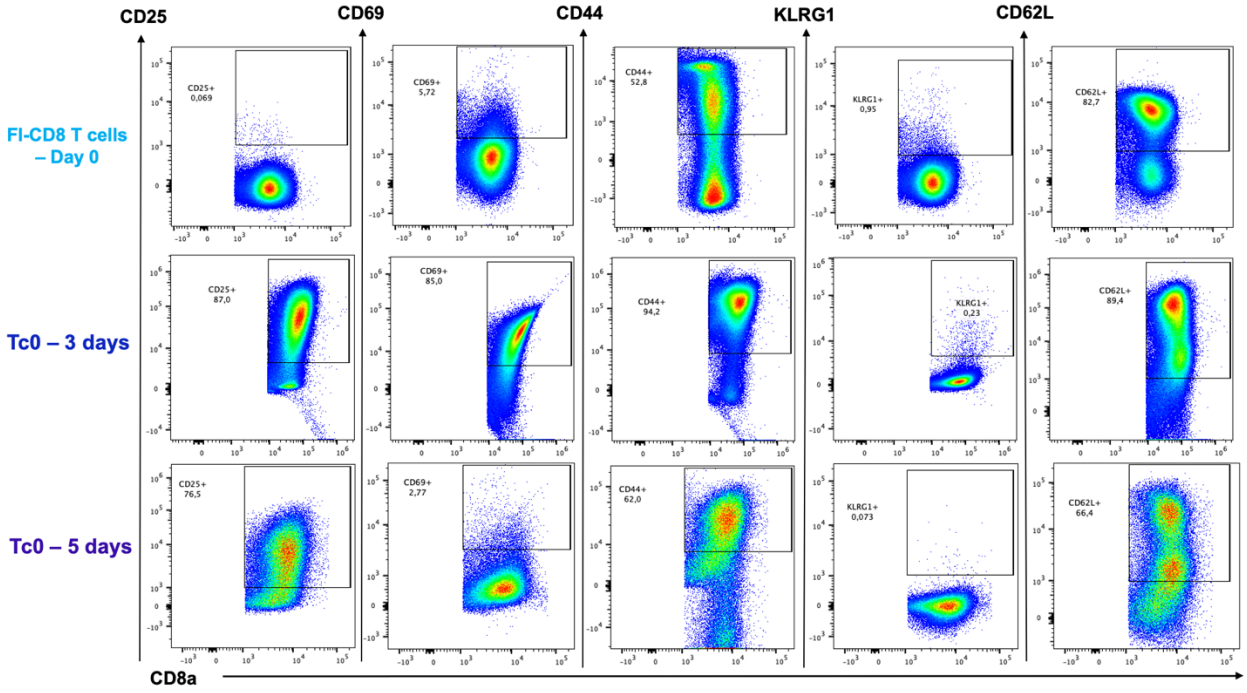

Figure 4: Comparison of CD8⁺ T cell activation profile after 3 and 5 day-culture. MFC pseudocolor plots of activation surface markers expressed by FI-CD8 T cells and activated-only cells (Tc0) from WT mice cultured in 24-well, flat-bottom plates for 3 or 5 days. Plots were gated on viable CD8a⁺ cells and reveal classical activation markers, CD69 and CD25, as well as other activation markers such as CD44, KLRG1 and CD62L, which can also determine the transition between effector and memory precursors, post activation. Plots are representative of independent experiments performed for all three populations.

First, viability was above 90% for both FI-CD8 T cells and Tc0 of 3-days culture. However, after 5 days in culture, stimulated Tc0 cells display a significantly lower viability (replicates mean ≈ 30%), perhaps as the result of chronic stimulation with anti-CD3/CD28 beads (AICD) or the absence of proper levels of survival factors, such as IL-2. In any case, when we gated on viable CD8T cells, Tc0 from both 3 and 5 day-culture displayed signs of activation, represented particularly by the expression of CD25, the high affinity IL-2 receptor (**Figures 4 and 5 A-B**). In comparison, as expected, FI-CD8 had no expression of CD25 (**Figures 4 and 5 A-B**). Interestingly, although the frequencies of CD25-positive cells were similar on days 3 and 5, the level of expression of CD25, as measured by the MFI, decreased on day 5 compared to day 3

(**Figures 4 and 5 A-B**). Similar upregulation on day 3 and downmodulation on day 5 also occurred for the expression of CD69, CD44, CD62L and CD8. In these cases, the percentage of positive events also decreased in 5 days (**Figures 4 and 5 A-B**). Unexpectedly, no KLRG1 expression were observed before or after stimulation (**Figures 4)**. Intriguingly, upon activation, two CD62L^{+} populations (high and low) were observed in both 3- and 5-day cultures (**Figures 4 and 5**).

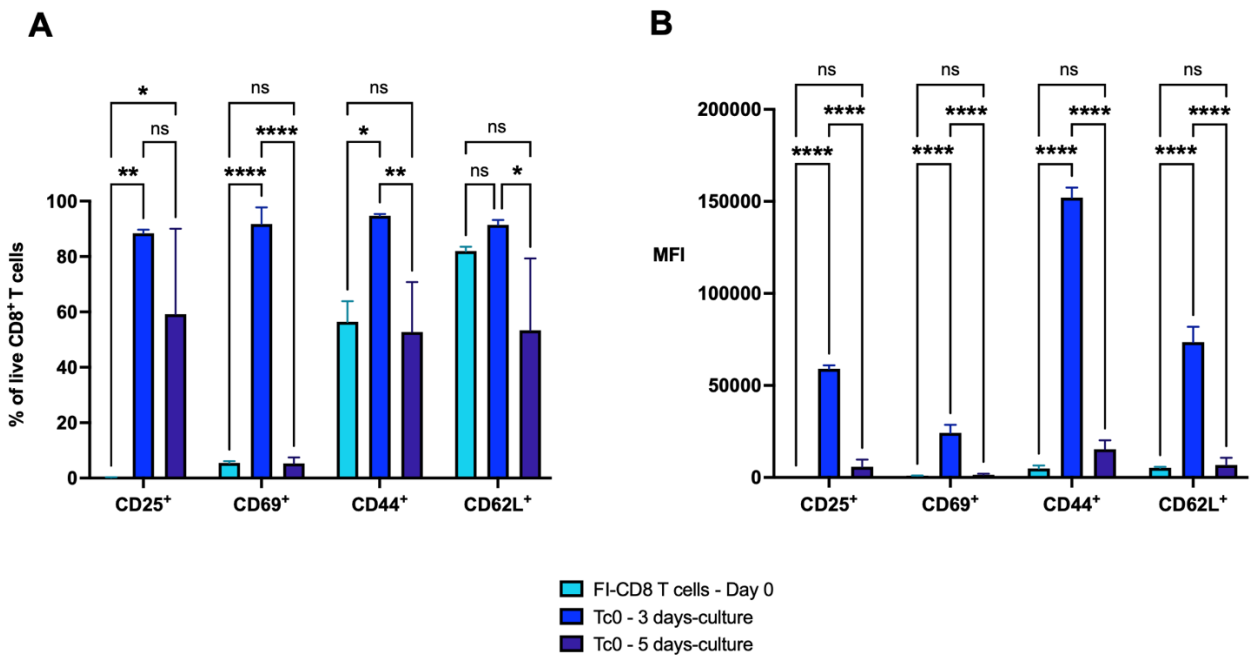

Figure 5: Frequency and Mean Fluorescence Intensity (MFI) of CD8^{+} T cells before and after activation. Statistical analysis of activation markers CD25, CD69, CD44 and CD62L, expressed by viable FI-CD8^{+} T and Tc0 cells from WT mice cultured in a 24-well~~,~~ flat-bottom plate for 3 and 5 days. **A)** % of CD8^{+} cells expressing the activations markers. **B)** MFI of CD8^{+} cells expressing the same activations markers. **(A-B)** ANOVA comparing samples from independent experiments performed for all three populations. Graphs show mean, standard deviation (SD) and multiple comparisons where: * = p<0.05, ** = p<0.01, *** = p<0.001 **** = p<0.0001 and ns = no significant. N = 3

Taken together, our results suggest that CD8^{+} T cells were being properly activated and that day 3 is the peak of activation in our experimental conditions.

$CD8^+$ T cell Differentiation towards Tc1 and Tc2

After establishing the best conditions to successfully activated $CD8^+$ T cells *in vitro*, we decided to study the differentiation towards Tc1 and Tc2, the two better described $CD8^+$ T cell effector subsets.

Again, we initiated by testing protocols and adjusting the levels of differentiating cytokines and blocking antibodies in our cultures. For that, 2 x 10^5/well of FI-CD8 T cells from WT animals were cultured for 3 days in 24-wells, flat-bottom plates containing IL-2, anti-CD3/CD28 magnetic beads, as well as IL-12 (Tc1), IL-4 and anti-IFN-γ antibody (Tc2). Tc0 was also generated with no polarizing cytokines and set as a negative control for the differentiation process. To confirm polarization, mRNA expression of specific genes for Tc1 (*Tbx21, Ifng* and *Il18r*) and Tc2 (*Gata3* and *Il4*) were analyzed by qPCR (**Figure 6 A-B**). As expected, Tc1 polarization was confirmed by increased mRNA levels of *Tbx21, Ifng* and *Il18r*, whereas Tc2 polarization resulted in upregulation of *Gata3* and *Il4* (**Figure 6 A-B**).

Activation profile of Tc1 and Tc2 effector cells

We further analyzed the effect of the polarizing conditions on the expression of the activation markers. Therefore, 2 x 10^5/well of FI-CD8 T cells from WT animals were cultured for 3 days in 24 flat-bottom well plates containing IL-2, anti-CD3/CD28 magnetic beads, as well specific cytokines, already mentioned, for Tc1 and Tc2 polarization. After culture period, cells were stained for selected activation markers (CD25, CD69, CD44, KLRG1 and CD62L) using extracellular staining protocol, and analyzed by MFC (**Figure 7**).

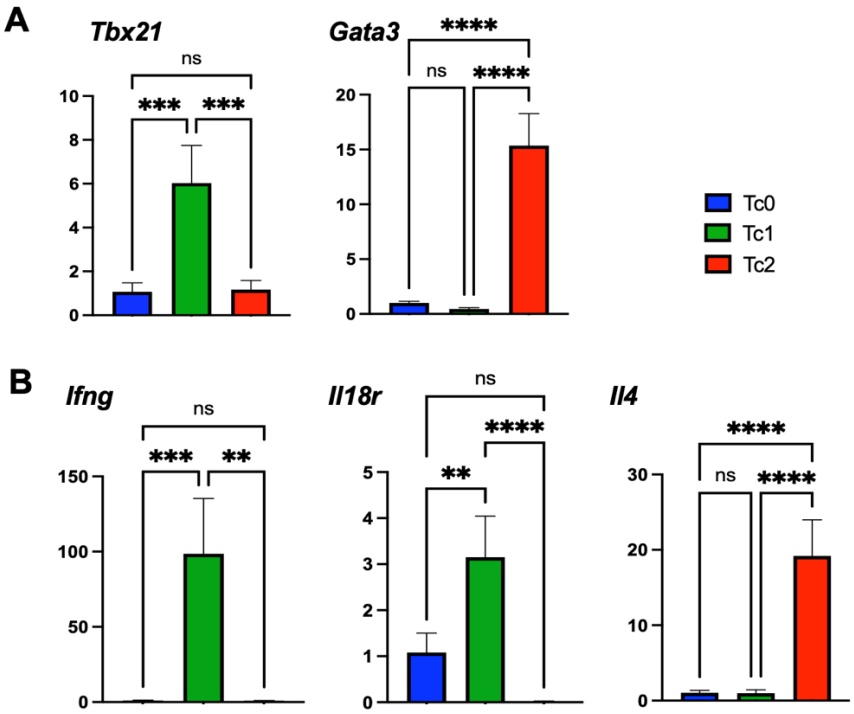

Figure 6: *In vitro* CD8⁺ T cell differentiation towards Tc1 and Tc2. mRNA expression analysis by qPCR of **A)** specific transcriptional factors genes *Tbx21* and *Gata3* and **B)** specific effector molecules genes *Ifng, Il18r* and *Il4* from WT animals cultured in 24-well, flat-bottom plates for 3 days. **(A-B)** mRNAs expression between *Actb* and other genes, in the three represented subsets, were previously compared to normalized all data. ANOVA of one independent experiment (representative of two independent experiments), showing mean, SD and multiple comparisons, where: ** = p<0.01, *** = p<0.001, **** = p<0.0001 and ns = no significant. N = 4.

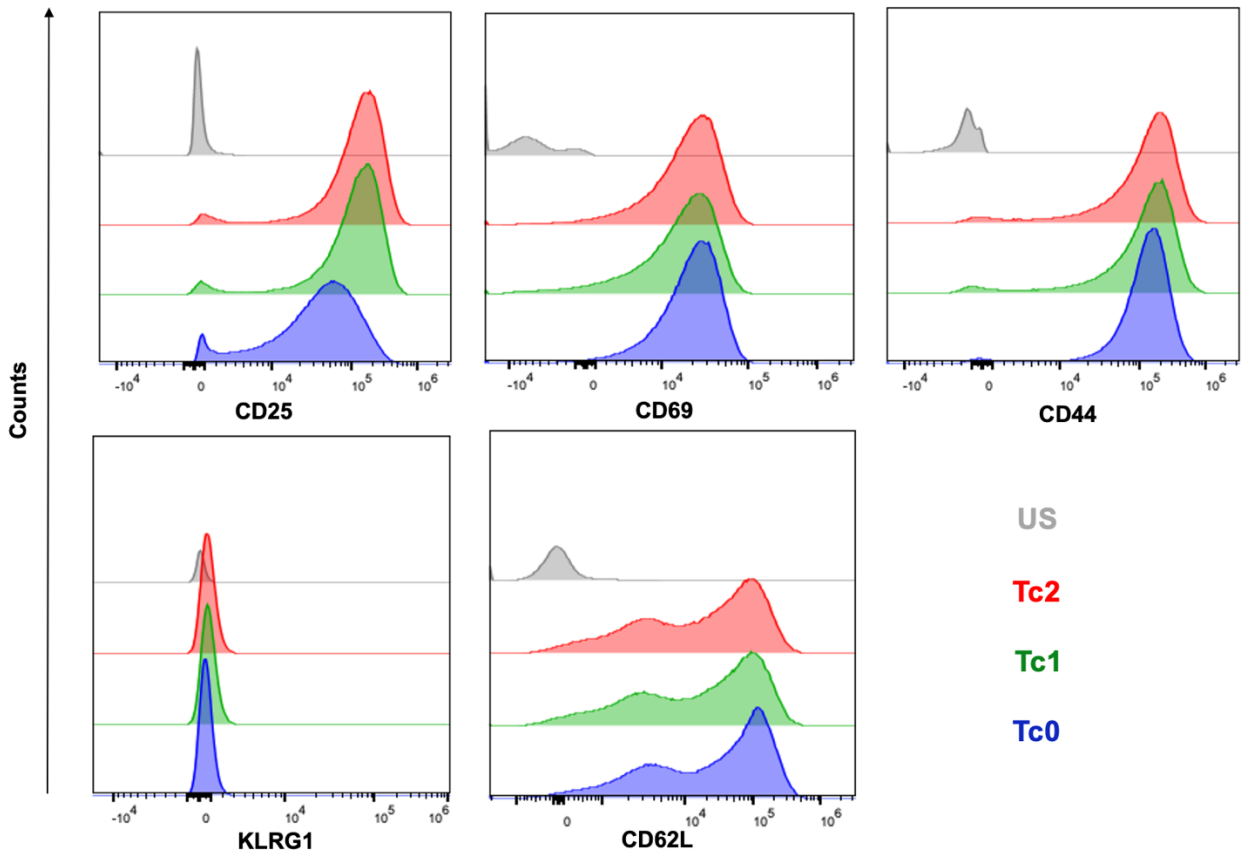

Figure 7: *In vitro* CD8⁺ T cell activation and differentiation. MFC histogram profiles of activated and differentiated subsets (Tc0, Tc1 and Tc2. US: unstained negative control) from WT mice cultured in 24-well flat-bottom plates for 3 days, gated on viable CD8a⁺ cells. Plots reveal the same group of activation markers previously mentioned (CD25, CD69, CD44, KLRG1 and CD62L) expressed by each cell subset.

All three subsets demonstrated viability superior to 90% after 3-day cultures. Also, all subsets presented increased expression of the activation markers when compared to unstimulated control, except KLRG1 (**Figure 7**). In addition, all three subsets presented similar frequency of CD69-, CD44- and CD62L-positive cells. Interestingly, Tc1 and Tc2 demonstrated increased frequency of CD25-positive cells compared to Tc0 (**Figure 8 A-B**). Moreover, the expression of CD25 was statistically higher in both Tc1 and Tc2, compared to Tc0 (as shown by MFI graph in **Figure 8 B**). Strickingly, CD62L levels were statistically lower in Tc2, compared to Tc1 and Tc0 **(Figure 8 A-B).**

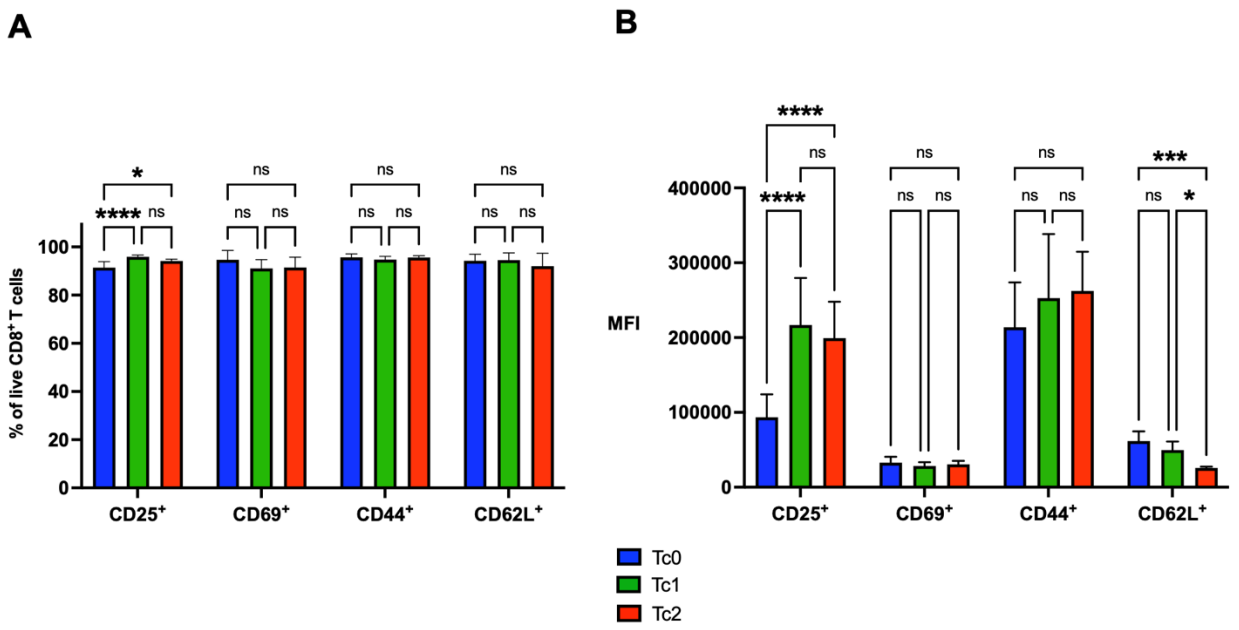

Figure 8: Frequency and MFI of surface marker-positive CD8⁺ T cells during *in vitro* activation and differentiation. Statistical analysis of **A)** Frequency (%) and **B)** MFI of viable CD8⁺ T cells expressing CD25, CD69, CD44 and CD62L by Tc0, Tc1 and Tc2 of WT animals after culture in 24 flat-bottom well plates for 3 days. ANOVA of three independent tests, showing mean, SD and multiple comparisons, where: * = p<0.05, *** = p<0.001 **** = p<0.0001 and ns = no significant. N =9

Furthermore, Tc1 and Tc2 also presented CD62L^{high} and CD62L^{low} populations, already shown for Tc0 during activation (**Figures 4, 7 and 9 A-B**). Remarkably, we observed that Tc0 and Tc1 histograms profiles were very similar for this molecule, but Tc2 cells presented a different profile (**Figure 9 A**). Tc2 presented lower levels of CD62L^{high} and higher levels of CD62L^{low} populations. Curiously, we found the MFI of CD62L^{high} subpopulations statistically different in Tc0, Tc1 and Tc2 cells, whereas no difference was observed for the MFI of CD62L^{low} subpopulations (**Figure 9 B**).

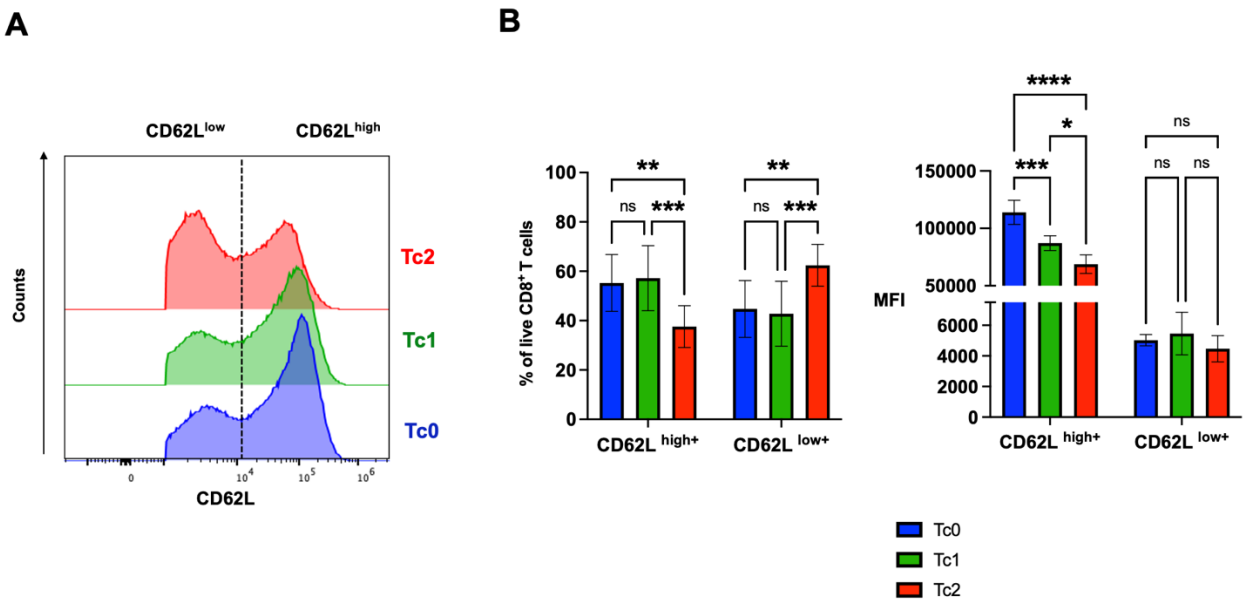

Figure 9: Expression of CD62L in CD8⁺ T cell subsets. Distinct expression of CD62L high and low populations by Tc0, Tc1 and Tc2 from WT mice, cultured in a 24-well flat-bottom plate for 3 days. **A)** MFC Histogram profiles showing different counts of CD62L high and low populations, gated on viable CD8a⁺ CD62L⁺ cells. **B)** Statistical analysis of Frequency (%) and MFI of viable CD8⁺ CD62L^{high+} and CD8⁺ CD62L^{high+} populations. ANOVA of three independent tests, showing mean, SD and multiple comparisons, where: * = p<0.05, ** = p<0.01, *** = p<0.001 **** = p<0.0001 and ns = no significant. N = 9

Expression of effector molecules by Tc1 and Tc2 effector cells

Finally, we evaluated the expression of effector molecules by Tc0, Tc1 and Tc2 subsets. Therefore, 2 x 10^5/well of FI-CD8 T cells from WT animals were cultured for 3 days in 24-well flat-bottom plates containing IL-2, anti-CD3/CD28 magnetic beads, as well as the specific polarizing cytokines as described above. After three days, cells were harvested and stained for selected effector molecules (IFN-γ, TNF-α, Granzyme B, Perforin, IL-4 and FasL (CD178)), using intracellular staining protocol, and analyzed by MFC.

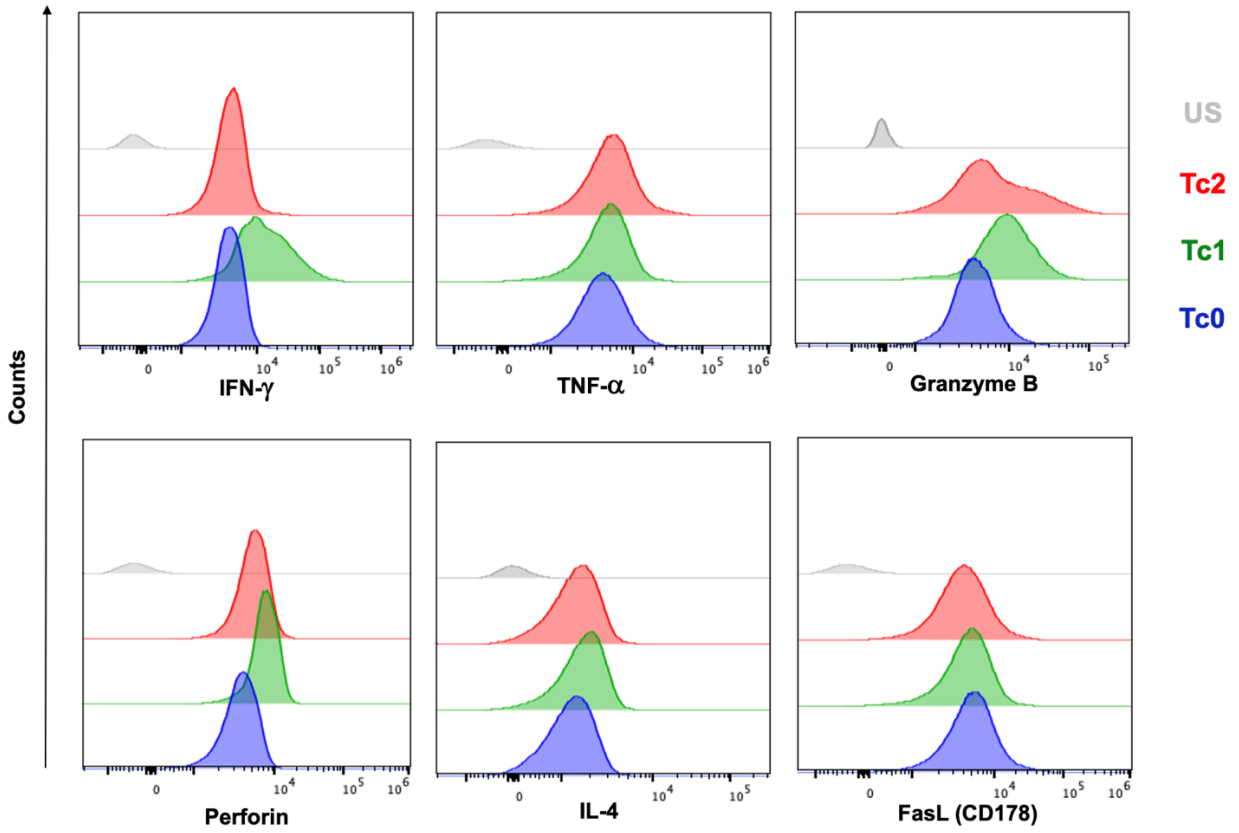

Figure 10: *In vitro* CD8⁺ T expression of effector molecules. MFC histogram profiles gated on viable CD8a⁺ cells demonstrating Tc0, Tc1, Tc2, expression of effector molecules related to these subsets (IFN-γ, TNF-α, Granzyme B, Perforin, IL-4 and FasL (CD178), from WT mice after 3 days culture in 24-well flat-bottom plates. US is also represented as a negative control.

All three subsets demonstrated increased expression of all the effector molecules assessed, compared to US (**Figure 10**). As expected, the frequency and expression levels of IFN-γ was statistically higher in Tc1 compared to Tc2. Moreover, expression levels of IFN-γ was also higher in Tc1 compared to Tc0 (**Figure 11 B**). These observations match our previous results from qPCR assay (**Figures 6, 10 and 11 A-B**). Surprisingly, there were no significant differences in frequency and MFI of TNF-α, IL-4 and Perforin among the three subsets (**Figure 11 A-B**). Moreover, Tc2 apparently presented some significant increase in frequency of FasL (CD178), compared to Tc1, but not compared to Tc0. (**Figure 11 A-B**).

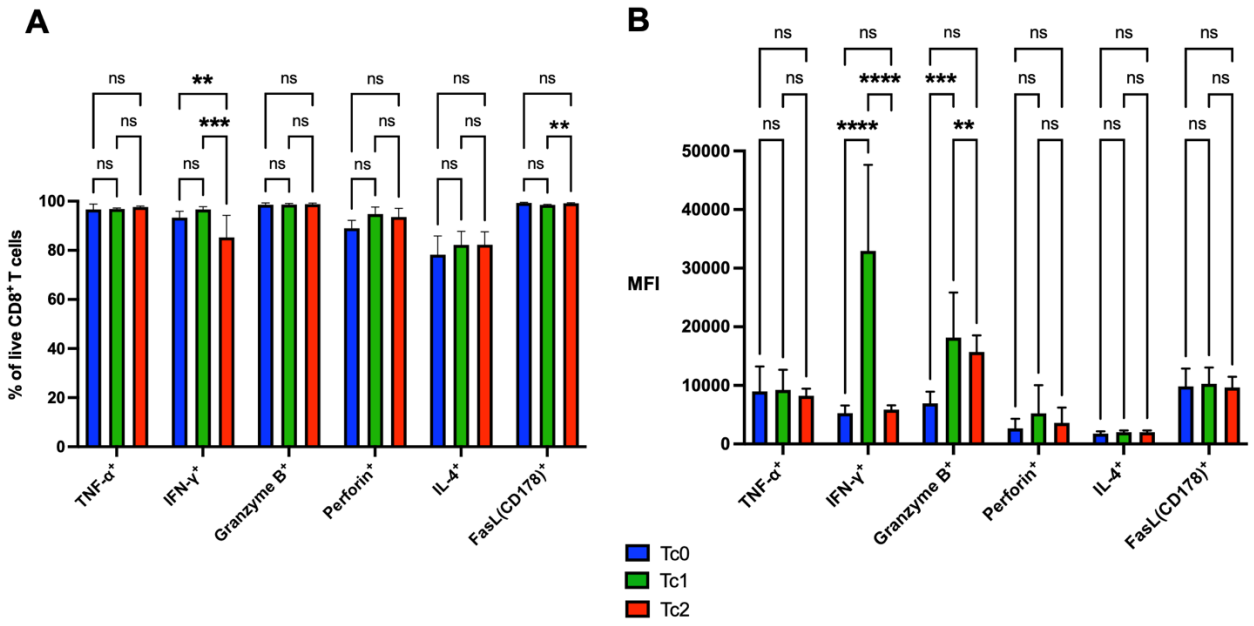

Figure 11: Frequency and MFI of CD8$^+$ T cells' effector molecules production during *in vitro* activation and differentiation, after 3 days-culture. Statistical analysis of **A)** Frequency (%) and **B)** MFI of viable CD8$^+$ T cells' production of IFN-γ, TNF-α, Granzyme B, Perforin, IL-4 and FasL (CD178) by Tc0, Tc1 and Tc2 from WT animals, after culture in 24 flat-bottom well plates for 3 days. ANOVA of two independent tests, showing mean, SD and multiple comparisons, where: ** = p<0.01, *** = p<0.001, **** = p<0.0001 and ns = no significant. N = 6

Regardless that all three subsets revealed high frequency of positive cells for granzyme B, with no statistical difference, Tc1 presented significantly higher MFI of granzyme B production compared to Tc0 and Tc2 (**Figure 11 A-B**). In combination, our results suggest that all three subsets are capable of performing effector activity. Importantly, higher frequencies of cells expressing IFN-γ and TNF-α or IFN-γ and Granzyme B at the same time, a characteristic of superior cytotoxic effector function, were found in the Tc1 subset (**Figure 12 A-B**).

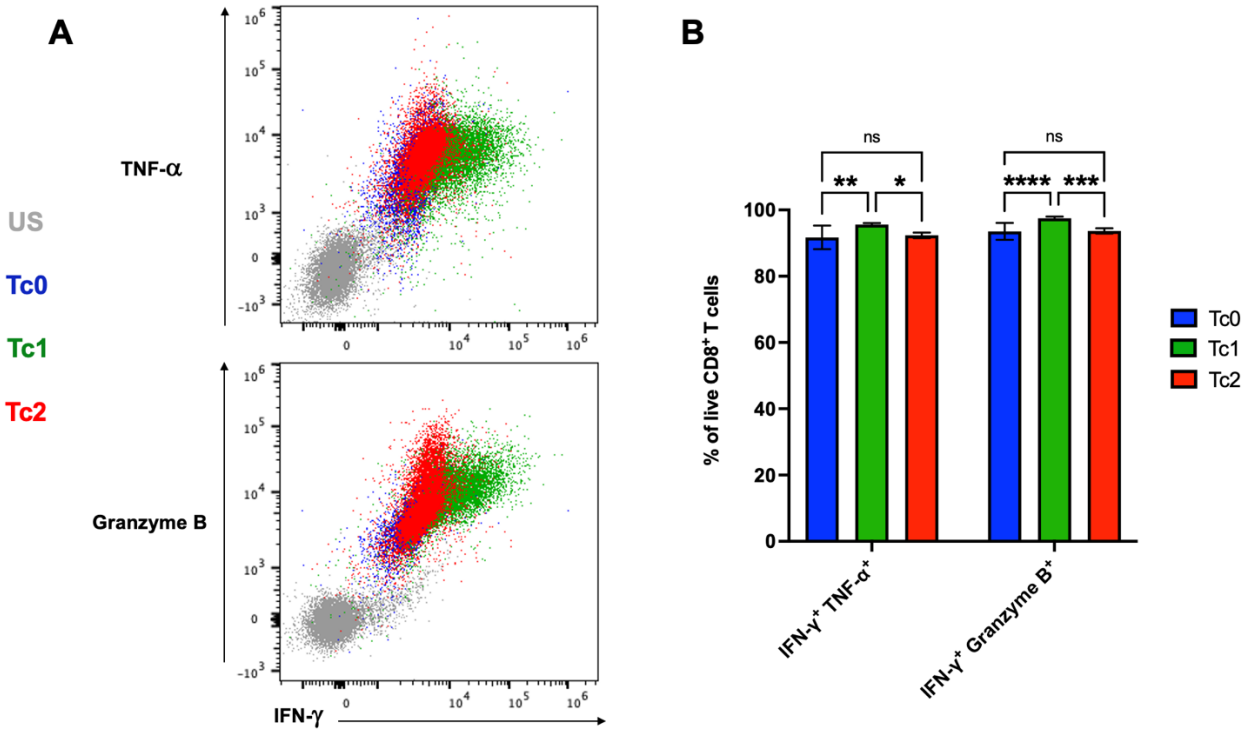

Figure 12: Assessment of Cytotoxic populations of CD8$^+$ T cells subsets after 3 days-culture. Viable CD8$^+$ T cells demonstrating Tc0, Tc1 and Tc2 double positive populations for production of IFN-γ and TNF-α (IFN-γ$^+$ TNF-α$^+$ cells), also production of IFN-γ and Granzyme B (IFN-γ$^+$ Granzyme B$^+$ cells), from WT mice cultured in 24 flat-bottom well plates for 3 days. **A)** MFC dot plots, where US is represented as a negative control. **B)** Statistical analysis of frequency (%) of double positive cells (IFN-γ$^+$ TNF-α$^+$ and IFN-γ$^+$ Granzyme B$^+$) of Tc0, Tc1 and Tc2. ANOVA of two independent tests, showing mean, SD and multiple comparisons, where: * = p<0.05, ** = p<0.01, *** = p<0.001, **** = p<0.0001 and ns = no significant. N = 6

Role of Fas/FasL interaction on Tc1 and Tc2 subset differentiation and function

After establishing and validating the conditions to differentiate Tc1 and Tc2 subsets, we investigate the effect of Fas/FasL interaction using FasL-deficient *gld* mice. First, we compared the expression of activation markers and effector molecules by FI-CD8 T cells from C57Bl/6 WT and *gld* mice. Regarding activation markers, as predicted, neither CD25 nor KLRG1 expression was observed in FI-CD8 T cells from both WT and *gld* (**Figure 13**). Also, a very small expression of CD69 was presented, which was statistically similar for both lineages in frequency and MFI

(**Figures 13 and 14 A-B**). Finally, CD62L and CD44 were highly expressed in both lineages and presented similar profiles (**Figures 13 and 14 A-B**).

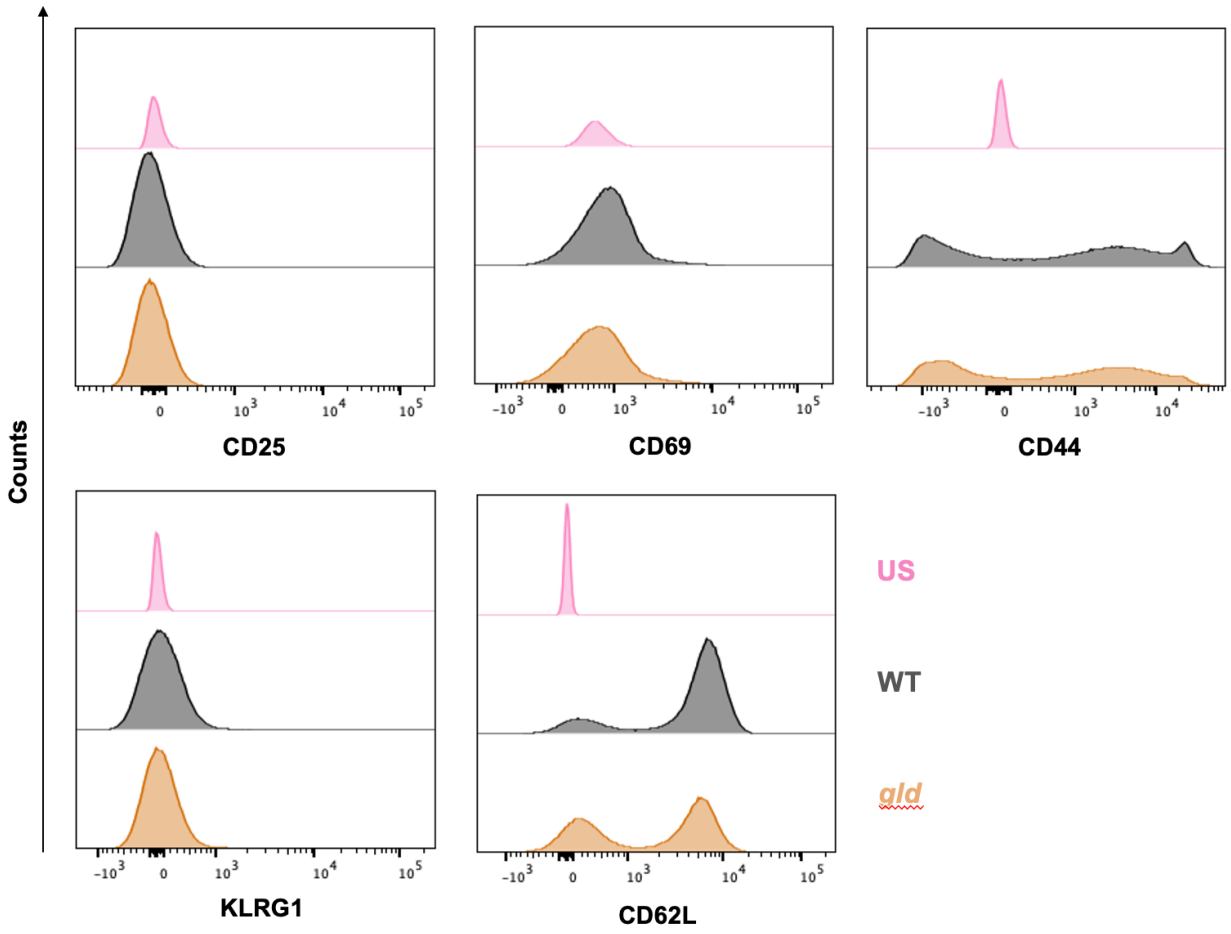

Figure 13: *In vitro* expression of activation markers FI-CD8 T cells from WT and *gld* mice. MFC histogram profiles (gated on viable CD8a^{+} cell) of activation markers (CD25, CD69, CD44, KLRG1 and CD62L), expressed by FI-CD8 T cells on Day 0 from WT and *gld* mice. US is represented as single negative control.

FI-CD8 T cells from *gld* mice also demonstrate two distinct CD44 populations (CD44^{high} and CD44^{low}), as previously observed for WT. Curiously, although similar in MFI, FI-CD8 T cells from *gld* mice display decreased frequency of CD44^{high} and increased frequency of CD44^{low} when

compared to WT mice (**Figures 4, 13 and 15 A**). These results indicate that FI-CD8 T cells from WT and *gld* mice display similar expression of activation markers.

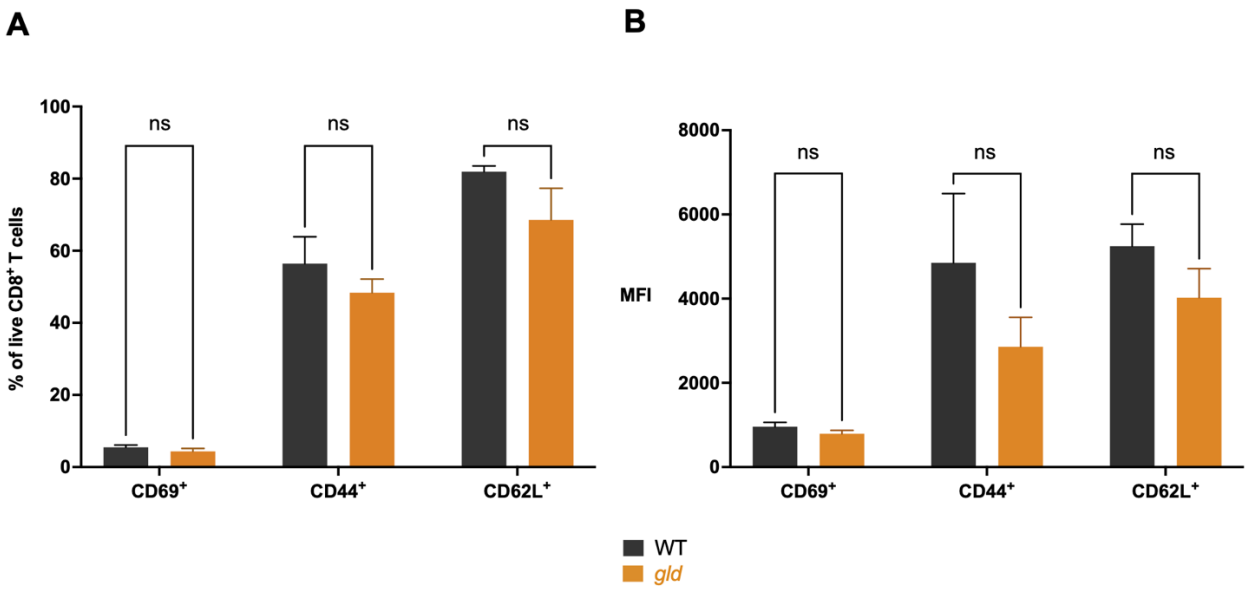

Figure 14: *In vitro* expression of activation markers FI-CD8 T cells from WT and *gld* mice. Statistical analysis of **A)** Frequency (%) and **B)** MFI of viable $CD8^+$ T cells expressing CD69, CD44 and CD62L by FI-CD8 T cells from WT and *gld* animals. T-test of one independent test, showing mean, SD and multiple comparisons, where: ns = no significant. N = 3

Regarding the expression of effector molecules, our data also shown similar profiles of FI-CD8 T cells from WT and *gld* mice, consistent with unprimed cells, which did not express the effector molecules IFN-γ, Granzyme B, Perforin, and FasL (with the exception for TNF-α) (**Figure 16**).

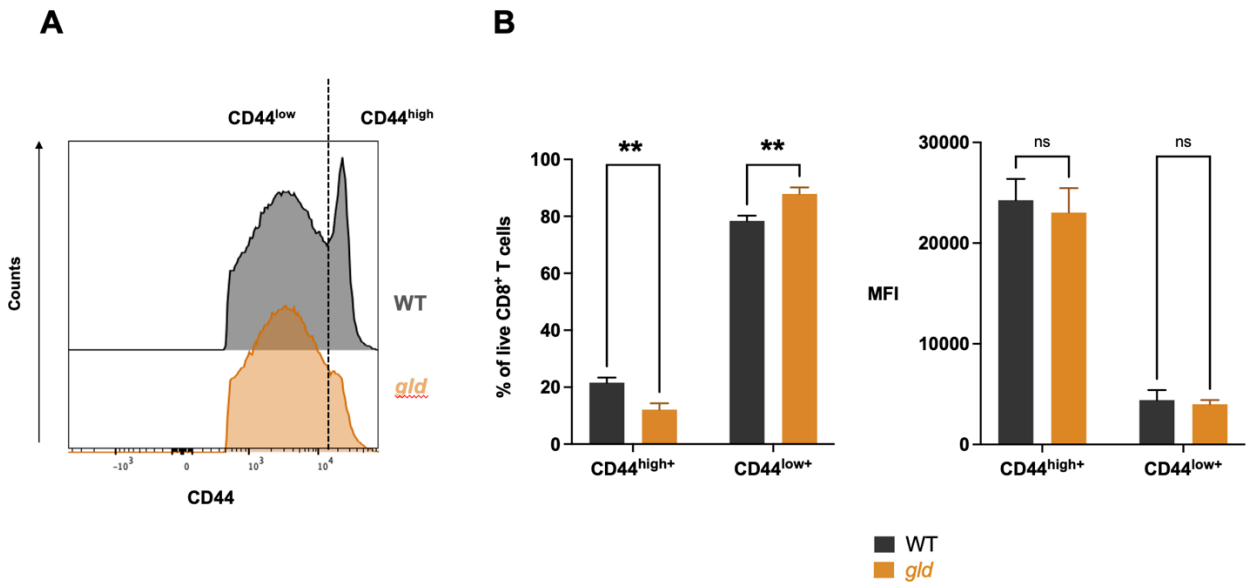

Figure 15: *In vitro* expression of CD44 by FI-CD8 T cells from WT and *gld* mice. Distinct *in vitro* expression of CD44 high and low populations by FI-CD8 T cells from WT and *gld* mice. **A)** MFC Histogram profiles showing different counts of CD44 high and low populations, gated on viable $CD8a^+$ $CD44^+$ cells. **B)** Statistical analysis of Frequency and MFI of CD44 high and low populations. T-test of one independent experiment showing mean, SD and multiple comparisons, where: ** = $p<0.001$ and ns = no significant. N=3

Next, we investigated the differentiation of FI-CD8 T cells from *gld* mice into Tc1 and Tc2, using the same protocol as described above. Tc0 was also generated with no polarizing cytokines and set as a negative control for the differentiation process. mRNA expression of specific genes for Tc1 (*Tbx21, Ifng* and *Il18r*) and Tc2 (*Gata3* and *Il4*) were analyzed by qPCR and revealed proper polarization of Tc1 and Tc2 subsets from *gld* mice (**Figure 17 A-B**).

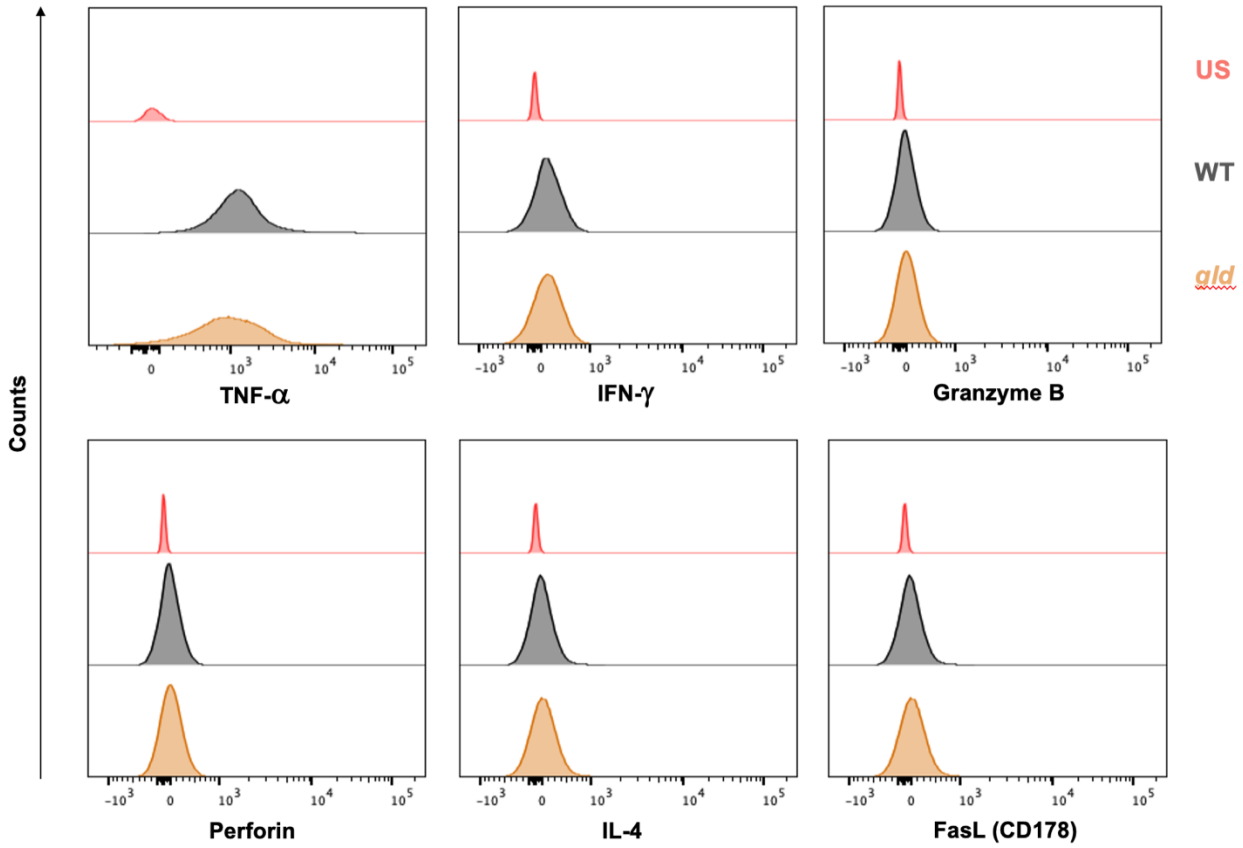

Figure 16: *In vitro* expression of effector molecules by FI-CD8 T cells from WT and *gld* mice Flow cytometry histograms profiles (gated on viable $CD8a^+$ cell) of effector molecules (IFN-γ, TNF-α, Granzyme B, Perforin, IL-4 and FasL(CD178)), produced by FI-CD8 T cells of WT mice compared to *gld* mice. US is represented as single negative control.

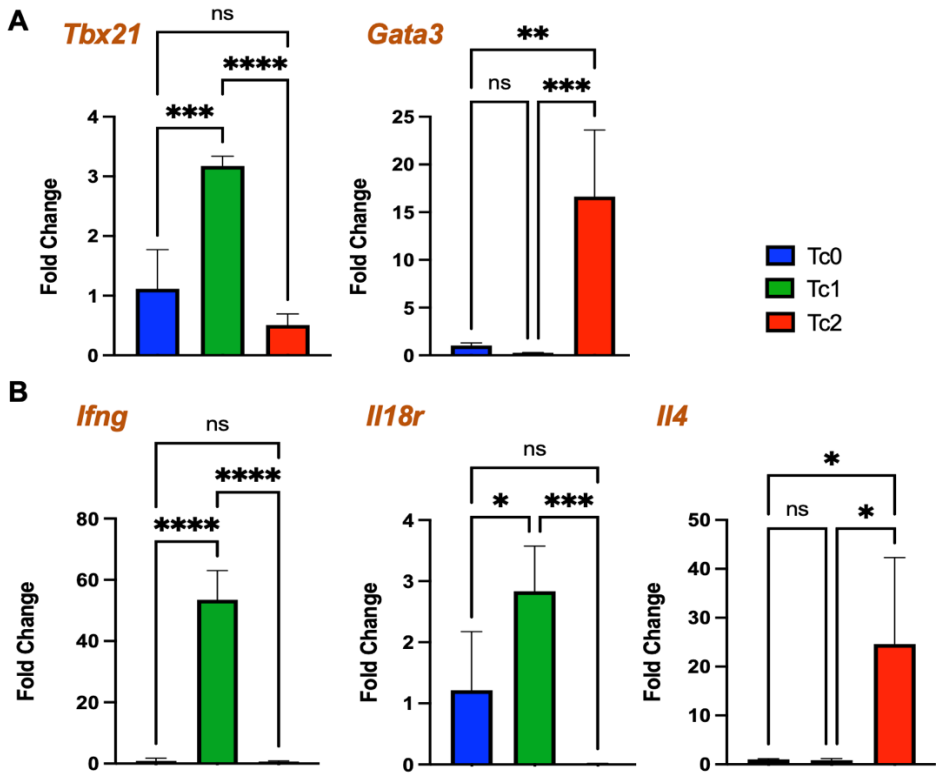

Figure 17: CD8⁺ T cells differentiation into Tc1 and Tc2 after 3 days-culture in *gld* mice. mRNA expression analysis by qPCR of **A)** specific transcriptional factors genes *Tbx21* and *Gata3* and **B)** specific effector molecules genes *Ifng, Il18r* and *Il4*, all related to CD8⁺ T cells differentiation in Tc1 and Tc2, after a 24 flat-bottom well plate culture for 3 days in *gld* animals. **(A-B)** mRNAs expression between *Actb* and other genes, in the three represented subsets, were previously compared to normalized all data. ANOVA of one independent test (also representative of two independent tests), showing mean, SD and multiple comparisons, where: * = p<0.05, ** = p<0.01, *** = p<0.001, **** = p<0.0001 and ns = no significant. N = 4

Next, we compared the activation profiles of Tc0, Tc1 and Tc2 from WT and *gld* mice. Using same polarization protocol, we evaluated the expression of selected activation markers (CD25, CD69, CD44, KLRG1 and CD62L) and observed similar frequency and MFI among the three subsets of WT and *gld* mice (**Figures 19 and 20**). The only exception was the frequency of CD69⁺ population of Tc2 cells, which was lower in *gld* compared to WT (**Figure 19**). Finally, the expression levels of CD62L were higher in Tc0 and Tc1 from *gld* compared to WT mice. (**Figure 20**).

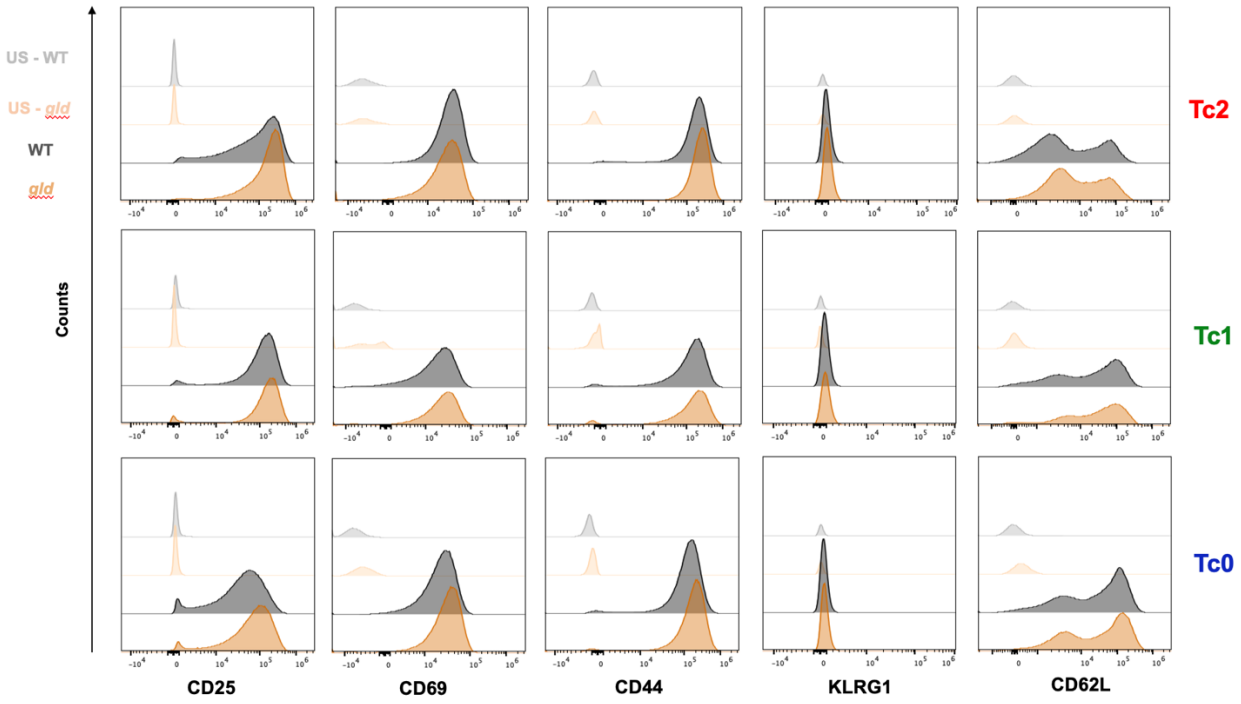

Figure 18: ***In vitro expression of*** **activation markers by Tc0, Tc1 and TC2 subsets from WT and** ***gld*** **mice.** MFC histograms (gated on viable $CD8a^+$ cell) of activation markers (CD25, CD69, CD44, KLRG1 and CD62L), expressed by each subset (Tc0, Tc1 and Tc2) of WT compared to *gld* mice, after culture in 24-well flat-bottom plates for 3 days. US – WT and US - *gld* are represented as negative controls of each correspondent lineage. $CD62L^+$ cells high and a low populations are also exhibited.

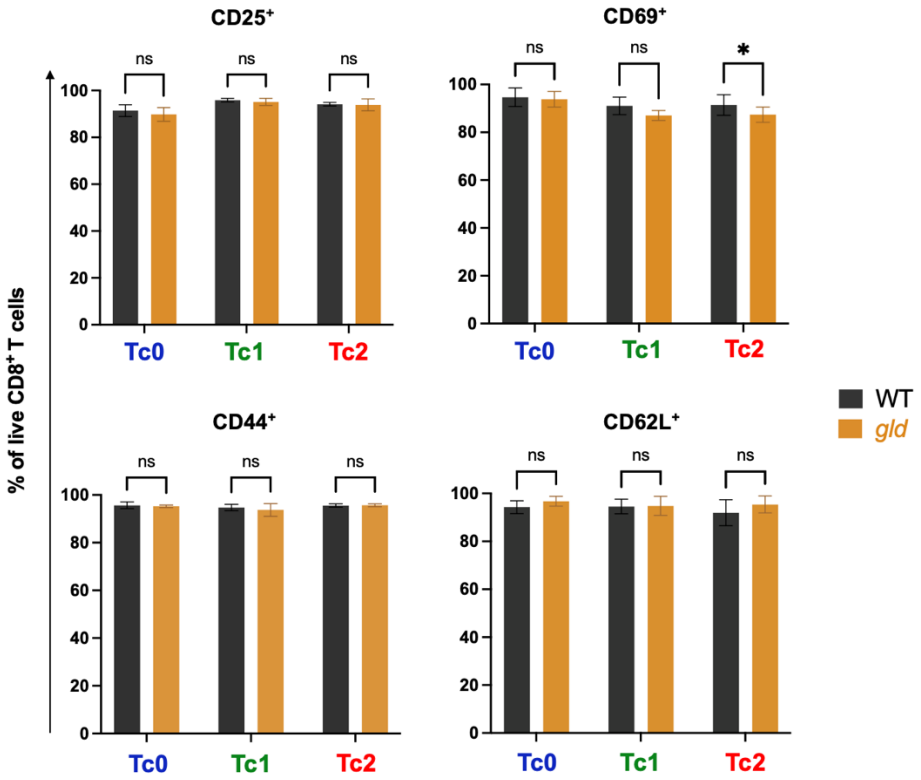

Figure 19: Frequency of activation markers-positive Tc0, Tc1 and Tc2 subsets from WT and *gld* mice. Statistical analysis of frequency (%) of viable $CD8^+$ T cells expressing CD25, CD69, CD44 and CD62L by Tc0, Tc1 and Tc2, of WT compared to *gld* animals, after culture in 24 flat-bottom well plates for 3 days. ANOVA of three independent tests, showing mean SD and multiple comparisons, where: * = $p<0.05$ and ns = no significant. N = 9

Interestingly, the frequency of $CD62L^{high}$ and $CD62^{low}$ positive cells were statistically higher and lower, respectively, in Tc1 cells from *gld* when compared to WT mice (**Figure 21B**). Moreover, both Tc0 and Tc1 cells from *gld* mice presented increased $CD62^{high}$ MFI compared to WT counterparts. In addition, Tc2 cells from *gld* mice displayed increased expression of $CD62L^{low}$, as assessed by the MFI, when compared to WT mice (**Figure 21 B**). Our results indicate that the absence of functional FasL does not significantly interfere with the activation of $CD8^+$ T cells.

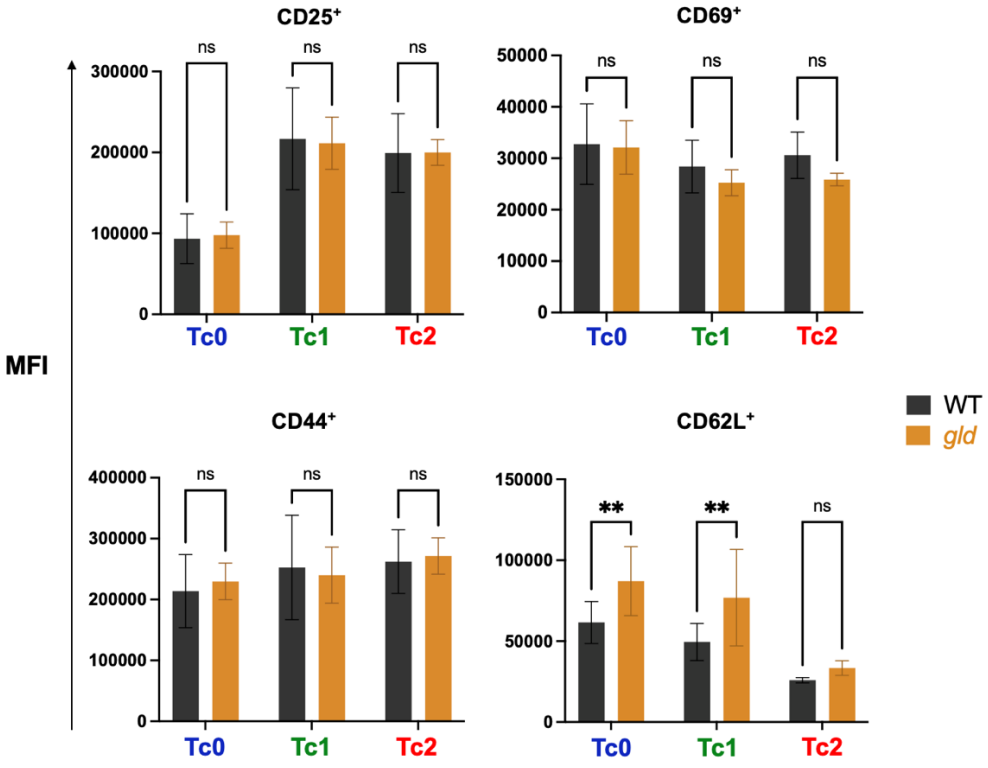

Figure 20: *MFI of* activation markers-positive Tc0, Tc1 and Tc2 subsets from WT and *gld* mice. Statistical analysis of MFI of viable $CD8^+$ T cells expressing CD25, CD69, CD44 and CD62L by Tc0, Tc1 and Tc2, of WT compared to *gld* animals, after culture in 24-well flat-bottom plates for 3 days. ANOVA of three independent tests, showing mean and SD, where: ** = $p<0.01$ and ns = no significant. N = 9

Lastly, we evaluated the role of FasL on the expression of effector molecules (IFN-γ, TNF-α, Granzyme B, Perforin, IL-4 and FasL) by Tc0, Tc1 and Tc2. Overall, there was no important difference in the expression of effector molecules by the $CD8^+$ T cell subsets of WT and *gld* mice (**Figures 22-24**), except for the level of IFN-γ, which was higher in Tc1 cells from *gld* mice.

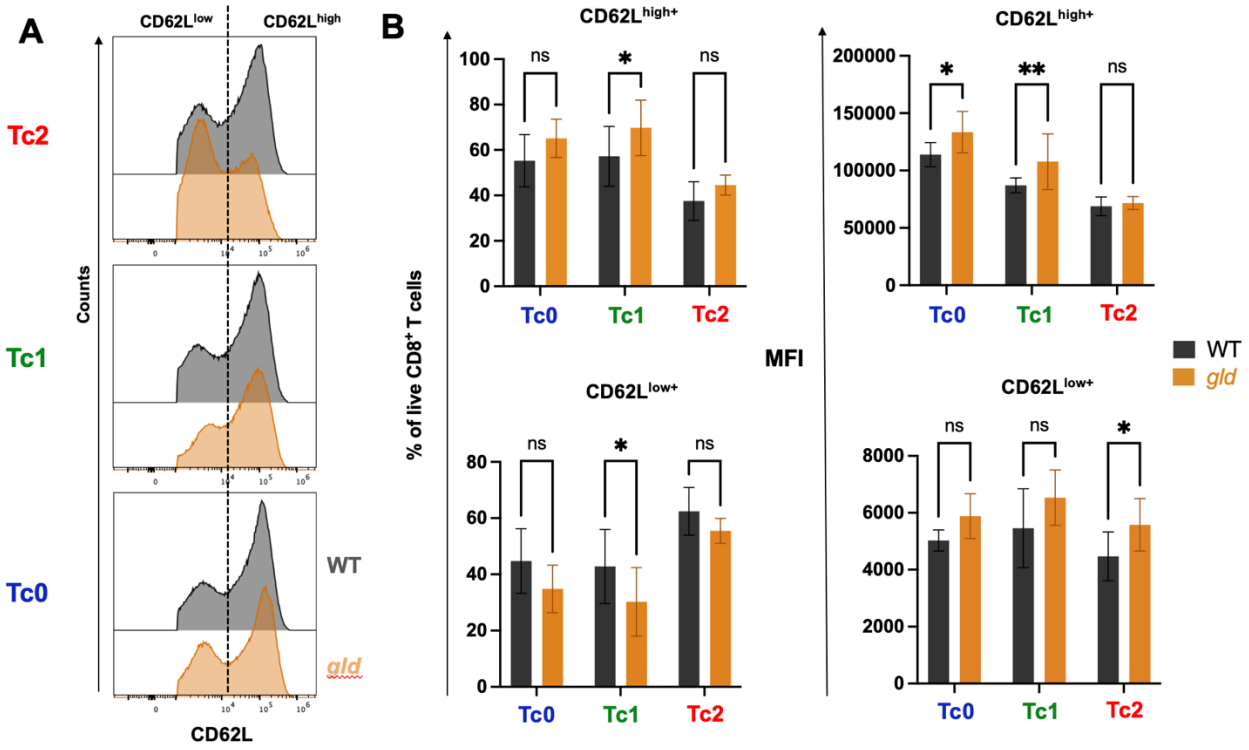

Figure 21: *In vitro* expression of CD62L by FI-CD8 T cells from WT and *gld* mice. Distinct *in vitro* expression of CD62L high and low populations by Tc0, Tc1 and Tc2 from WT compared to *gld* mice, cultured in a 24 flat-bottom well plate for 3 days. **A)** MFC Histogram profiles showing different counts of CD62L high and low populations, gated on viable $CD8a^{+}$ $CD62L^{+}$ cells. **B)** Statistical analysis of frequency (%) and MFI of viable $CD8^{+}$ $CD62L^{high+}$ and $CD8^{+}$ $CD62L^{high+}$ populations. ANOVA of three independent tests, showing mean, SD and multiple comparisons, where: * = $p<0.05$, ** = $p<0.01$ and ns = no significant. N = 9

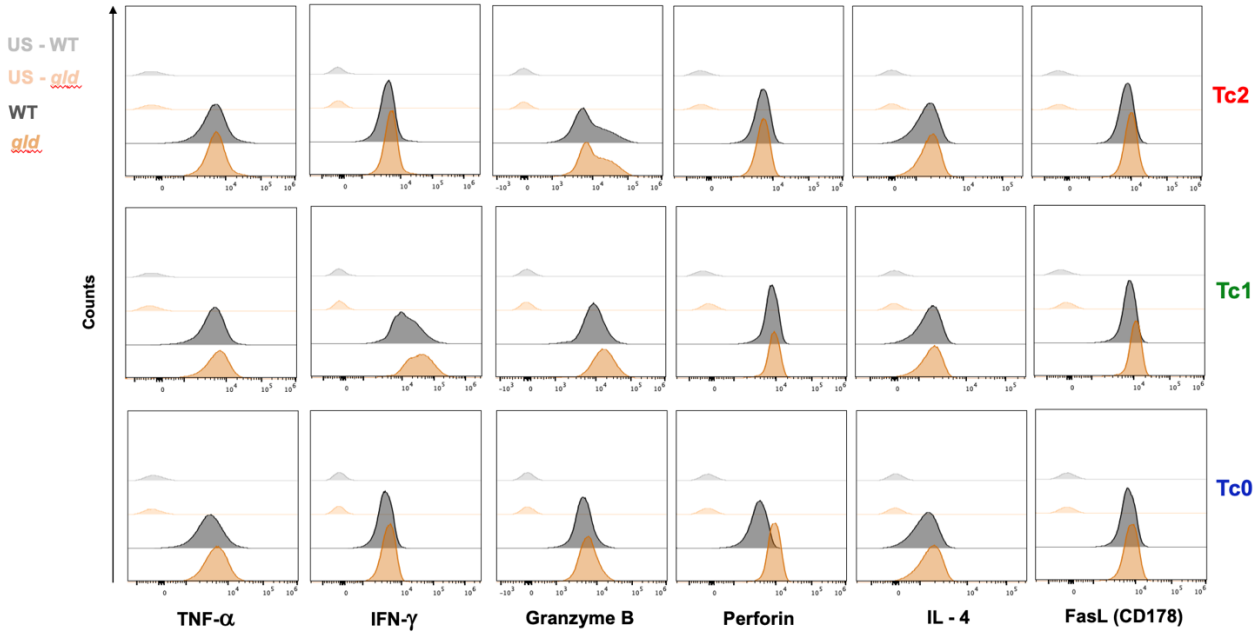

Figure 22: *In vitro expression of* effector molecules by Tc0, Tc1 and Tc2 subsets from WT and *gld* mice. MFC histograms (gated on viable CD8a$^+$ cells) showing the expression of effector molecules (IFN-γ, TNF-α, Granzyme B, Perforin, IL-4 and FasL) by Tc0, Tc1 and Tc2 of WT compared to *gld* mice, after culture in 24-well flat-bottom plates for 3 days. US – WT and US - *gld* are represented as negative controls of each correspondent lineage.

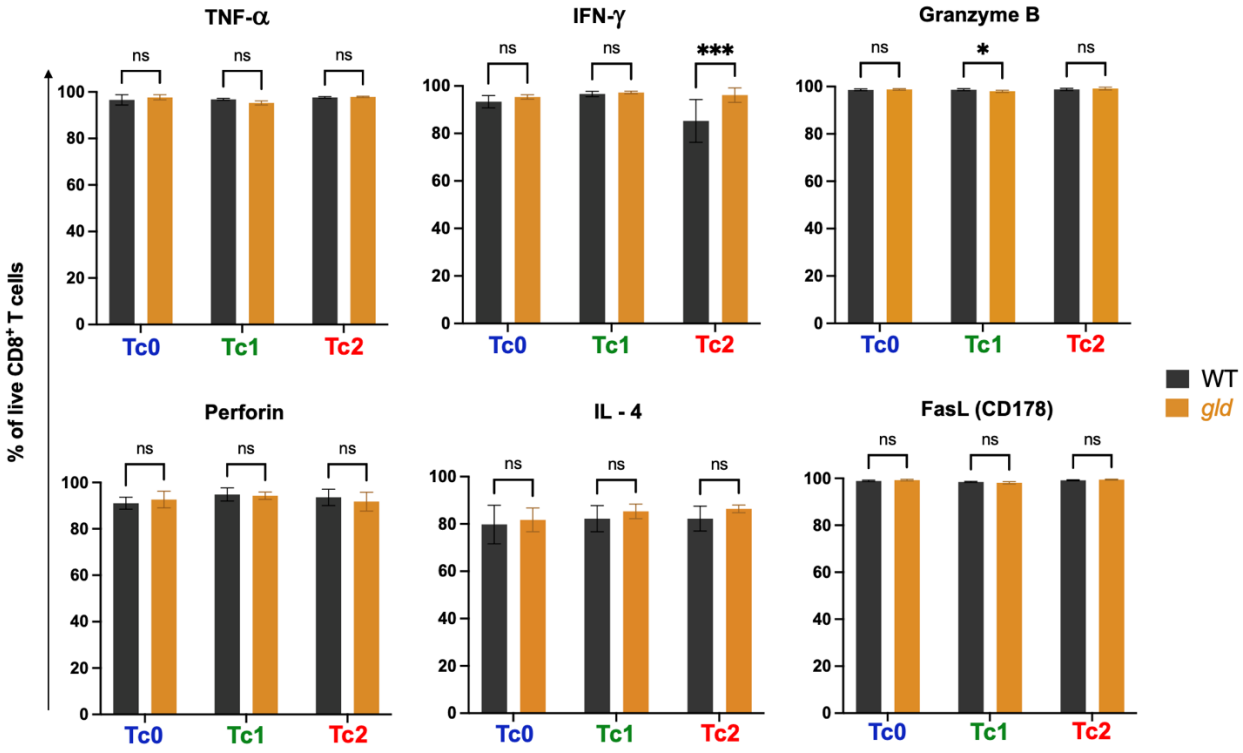

Figure 23: ***Frequency of effector molecules expressed by Tc0, Tc1 and TC2 subsets from WT and gld mice.*** Statistical analysis of Frequency (%) of viable $CD8^+$ T cells producing IFN-γ, TNF-α, Granzyme B, Perforin, IL-4 and FasL (CD178) by Tc0, Tc1 and Tc2, of WT animals compared to *gld*, after culture in 24 flat-bottom well plates for 3 days. ANOVA of two independent tests, showing mean, SD and multiple comparisons, where: * = $p<0.05$, *** = $p<0.001$ and ns = no significant.

N = 6

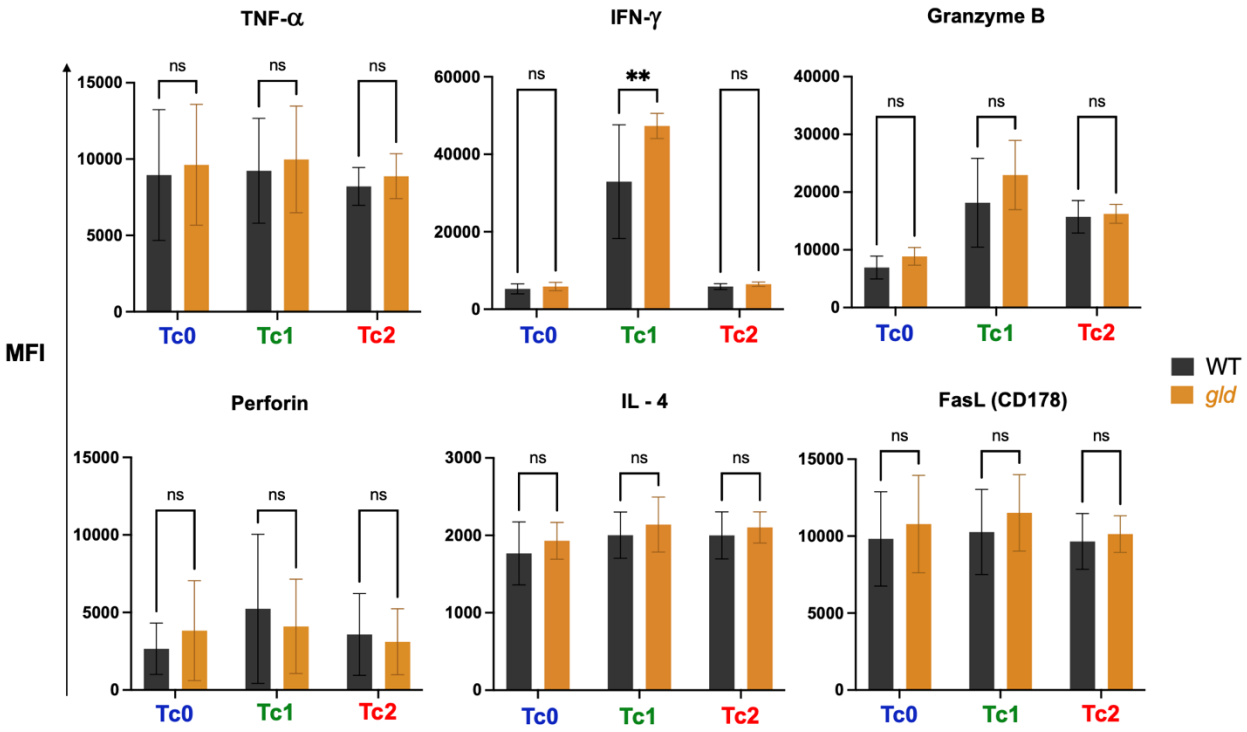

Figure 24: *In vitro expression of* effector molecules by Tc0, Tc1 and TC2 subsets from WT and *gld* mice. Statistical analysis of MFI of viable $CD8^+$ T cells producing IFN-γ, TNF-α, Granzyme B, Perforin, IL-4 and FasL (CD178) by Tc0, Tc1 and Tc2, of WT animals compared to *gld*, after culture in 24 flat-bottom well plates for 3 days. ANOVA of two independent tests, showing mean SD and multiple comparisons, where: ** = $p<0.001$ and ns = no significant. N = 6

Finally, we examined whether Tc0, Tc1 and Tc2 from *gld* mice were able to concomitantly produce two effector molecules, such as WT mice. We observed no significant differences between Tc0, Tc1 and Tc2 subsets from *gld* and WT mice (**Figures 25 and 26**). Taken together, our results indicate that the lack of functional FasL do not interfere in the expression of effector molecules by Tc0, Tc1 and Tc2 subsets.

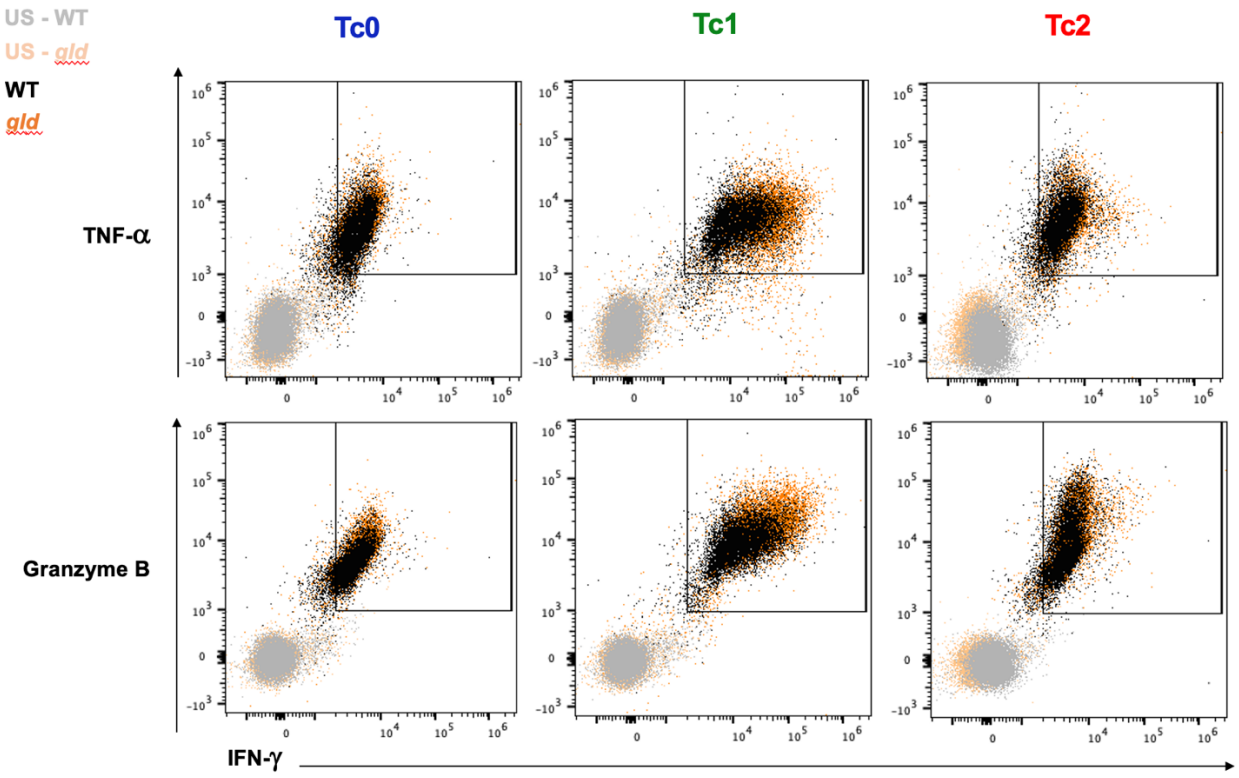

Figure 25: Assessment of cytotoxic populations of CD8⁺ T cells subsets. MFC dot plots gated on viable CD8⁺ T cells. Plots show Tc0, Tc1 and Tc2 double positive populations (IFN-γ⁺ TNF-α⁺ and IFN-γ⁺ Granzyme B⁺) of WT compared to *gld* mice, after culture in 24 flat-bottom well plates for 3 days. US - WT and US - *gld* are represented as negative controls of each correspondent lineage.

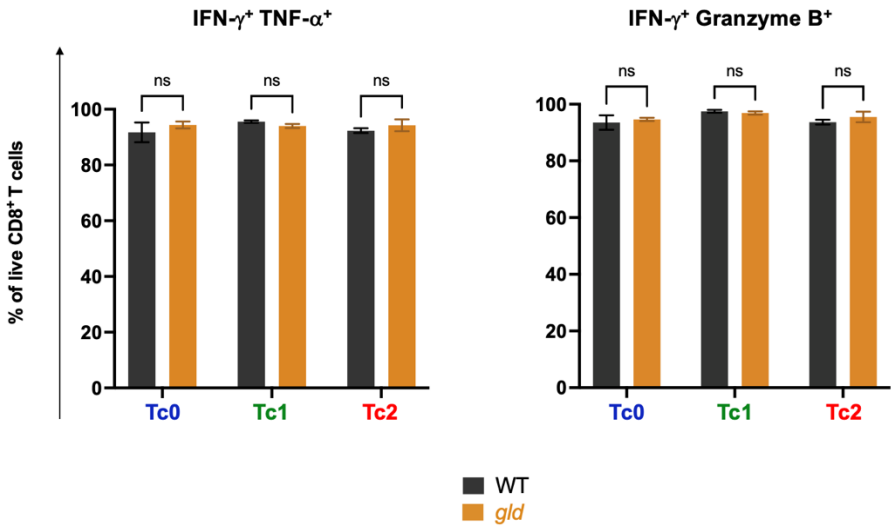

Figure 26: Comparison of the frequency of IFN-γ/TNF-α$^+$ and IFN-γ/Granzyme B$^+$ double positive CD8$^+$ T cells in WT and *gld* mice. Statistical analysis of frequency (%) of viable CD8$^+$ double positive cells (IFN-γ$^+$ TNF-α$^+$ and IFN-γ$^+$ Granzyme B$^+$) of Tc0, Tc1 and Tc2 from WT animals compared to *gld*. ANOVA of two independent test, showing mean, SD and multiple comparisons, where: ns = no significant. N = 6

5. Discussion

CD8$^+$ T cell activation

As previously mentioned, CD69 and CD25 have been widely reported to be classical activation surface markers of both CD4$^+$ and CD8$^+$ T lymphocytes [10–15]. CD25, as being the high affinity IL-2R alpha chain, is early expressed following engagement of TCR/CD3 and CD28 costimulatory signal and maintained expressed constitutively, as IL-2 is a crucial cytokine for T cells survival [11,98–100]. As expected, CD25 was expressed both on days 3 and 5 post stimulation. Interestingly, not only increased frequencies of CD25-positive cells were observed among Tc1 and Tc2 cells, compared to Tc0 cells, but the expression level of CD25 was also higher on the surface of Tc1 and Tc2 cells, as measured by MFI. In addition, CD69 is also an early activation marker, only transiently expressed after TCR and costimulatory signaling [101,102] . Accordingly, our results showed that the expression of CD69 was similarly upregulated by all subsets in both WT

and FasL-deficient animals after stimulation for 3 days and then downregulated again on day 5. Also, it has already been demonstrated that CD69 is only later expressed specifically in T_{RM} post infection [65,93,94,103].

The role of CD44 has been described not only as to mark the transient relation between effector and memory T cells, but also as an important molecule for function and maintenance of T cell homeostasis. CD44 has been directly associated with T cell trafficking, encounter with the antigen, for tissue migration after antigen exposure and more vital for memory precursors survival, being expressed in T cells from naïve to effector and memory subsets post activation in higher levels [18,19]. This concept matches our findings in which CD44 was expressed by most of our FI-CD8 T cells population and also by all *in vitro*-activated and -differentiated $CD8^+$ T cells subsets, from both mouse strains. The appearance of CD44 high and low events among FI-CD8 T cells could indicate that these cells may be composed of relatively heterogeneous populations. Although our mice were maintained in germ-free conditions, this could be the consequence of some antigenic activation related to food antigens and/or microbiota. Alternatively, this could represent different time points after thymic emigration.

It is well established that CD62L, or *L-selectin*, is a crucial molecule for naïve T cells entry into secondary lymphoid organs and that its expression is downregulated right after TCR/CD3 and CD28 signaling, when they procced to become effector cells [104]. Additionally, over the past two decades, CD62L has been extensively described as a vital molecule for T cell memory precursors, in special T_{CM}, being highly re-expressed due to their secondary lymphoid organs immunosurveillance activity that requires them to be re-exposure to the antigen inside those organs [104,105] . Moreover, effector T cells have been associated to a low expression of CD62L ($CD62^{low}$ population), while a high expression of CD62L ($CD62L^{high}$) is related to central memory cells [106–108] . In our first set of results, we observed significantly higher expression of CD62L by Tc0 obtained after 3 days in culture, compared to FI-CD8 T cells. In addition, we observed similar frequency of CD62L-positive Tc0, Tc1 and Tc2 cells obtained from WT mice. However, looking

strictly at CD62L expression, Tc2 demonstrated a more prominent effector behavior than Tc0 and Tc1, due to its higher percentage of $CD8^+$ T cells expressing $CD62L^{low}$ and at the same time, downregulation of CD62L per cell.

KLRG1 has been described as an effector marker of short-lived cells, expressed during infections [93], implicating that perhaps, an *in vitro* culture with no inflammatory stimuli might not show any expression of KLRG1. Another possibility that might explain no KLRG1 expression in our samples is that the conjugated antibody we used to detect $KLRG1^+$ cells could not be working appropriately during all staining tests. Unfortunately, due to lack of KLRG1-positive control samples, we were not able to test this theory. Nevertheless, further investigation through kinetics assay using a positive control could be an alternative to explore further.

FasL-deficient mice (*gld*) was described as a strain that holds a point mutation in the *C-terminal* of FasL molecule, the most conservative region within TNF-family members. This mutation generates loss of function - but no expression downregulation - which interferes with the binding to Fas receptor [109,110]. Some recent reports have associated *gld* mice to immunological responses in the Central Nervous System (CNS) and protective activity against viral infections, metastasis of lung cancer and lymph node graft-versus-host-disease [111–113]. However, we were not able to find any literature regarding the effect of FasL-deficiency specifically related to the expression of the activation markers in $CD8^+$ T cells.

In overall, our findings could not identify any statistically significant difference between *gld* and WT mice related to the expression of CD25, CD44 and CD69 (with the exception of frequency of $CD69^+$ Tc2 cells and frequency of CD44 high and low populations of FI-CD8 T cells). Although, it is very important to point out that from statistical point of view that the various means differences observed in **Figures 14, 19** and **20** trended to be different, despite no statistical significancy. This might implicate that FasL-deficiency reduces those activation markers when compared to a normal condition. Nonetheless, further testing is necessary, perhaps increasing sample size (N), which could reduce SD, allowing better analysis of significancy.

On the other hand, FasL-deficiency seems to interfere significantly with CD62L expression of high and low populations, generating different behavior of effector/memory when compared to a normal condition. More specifically, the lack of FasL functionality *in vitro* might shift $CD8^+$ T subsets more towards a memory-like behavior, increasing not only frequency of $CD62L^{high}$, but also the expression per cell of both high and low populations. This observation was only significant for Tc1, but also represented by means differences for both Tc0 and Tc2. Nevertheless, further investigation should be considered.

Expression of $CD8^+$ T cell Effector Molecules

Despite FI-CD8 T cells being a heterogenous population, it is composed mostly by naïve cells. This concept matches our results, in which no production of effector molecules (except of TNF-α) was revealed. However, curiously, FI-CD8 T cells in both lineages, presented increased percentages of TNF-α production. Even though we used very young animals to reduce antigen-exposure, it is reasonable to believe that little exposure had occurred prior to euthanasia, which also explain the heterogeneity feature of FI-CD8 T cells and eventually the observed TNF-α production.

As previously discussed, the knowledge of $CD8^+$ T cell differentiation in effector subsets is still under development, but it has already been widely and recently reported the relationship between transcription factors (*T-bet*, *GATA 3*, *RORγT*, etc), the production of effector molecules (Granzyme B and Perforin) and cytokines such as IFN-γ, TNF-α, IL-4, IL-9, IL-17, IL-22, as crucial to characterize effector subsets [26,34]. T-bet and IFN-γ have already been shown to be respectively the transcription factor responsible for differentiation to Type 1 effector subset and the specific cytokine produced by these cells. This matches our findings of statistically significant higher expression of *Tbx21* and IFN-γ production by Tc1 from both lineages, after 3 days-culture,

confirming the type 1 polarization. Also, the high expression of IL-18R in Tc1 already reported [26] was also confirmed in our 3 days culture mRNA analysis.

Similarly, Type 2 T cells are polarized in the presence of IL-4 that promotes *GATA 3* signaling and consequently increased production of IL-4, IL-5, and IL-13, and lower production of IFN-γ[26,41–44]. Our findings demonstrated higher expression of *GATA-3 and* IL-4 mRNAs by Tc2, as well as low IFN-γ mRNA, frequency and MFI, in both lineages, which is consistent with Tc2 polarization. Interestingly, *Il4* promoter region in Th2 from WT animals has been shown to be down-regulated by a microRNA (mir155), resulting in decreased expression of *Il4* and subsequently low production of IL-4 [114] .This could be an explanation to why Tc2 from both lineages, despite higher *il4* mRNA expression did not present significantly higher frequency and MFI of IL-4 production, we observed after 3 days culture. Another possible explanation would be the intrinsic IL-4 production kinetics, being a very-early-produced cytokine. Nonetheless, further investigation into kinetics and microRNA downregulation would be desirable.

TNF-α is known to be a key pro-inflammatory cytokine, in which production has also been demonstrated to be increased in Type 1 effector T cells, however it has been also reported production of TNF-α by Tc2 *in vitro* [115]. In addition, the production and secretion of TNF-α has been shown to be very quick, following TCR/CD3 and CD28 engagement [116,117] . Regardless the high frequency of TNF-α observed in Tc1, we found equally production in Tc1 compared to the other subsets, specially Tc2. One plausible explanation could be that during 3 days-culture period TNF-α was being released into the supernatant. In this case, even though TNF-α inside organelles was similar among subsets, levels of soluble TNF-α in the medium could be higher in Tc1 compared the other subsets. This explanation could also be applied for IL-4, which is also released to the medium and promptly consumed by Tc2. In any case, further experiments using ELISA to analyze supernatant content of each subset should bring more insights. Furthermore, we also believe that, despite each subset differentiation being placed individually in each culture-

well containing their specific cytokines, no polarization protocol drives 100% differentiation towards the desired phenotype.

Over the past decades, both granzyme B and perforin have also been profoundly studied and reported as effector molecules that promotes cytolytic and cytotoxic capacity to effector $CD8^+$ T cells, and their secretion associated to Type 1 T cell function [30,118]. Regardless similar percentage of granzyme B^+ among the three subsets, Tc1 revealed significantly the highest production of granzyme B per cell, matching this concept. Although, our findings revealed no significant distinction in levels of Perforin production among the three subsets.

The relationship among IFN-γ, TNF-α and cytolytic molecules in $CD8^+$ T cells effector function has been described to promote better quality of T cell response to an antigen, in which a dual activity, improves cytotoxic function and killing capacity [119]. Thus, the importance of TNF-α^+ IFN-γ^+, also IFN-γ^+ $Granzyme^+$ double-positive cells have been reported to be associated with many infectious diseases clearance[120], with the TME immune response [121] and even with metabolic diseases [122] . Regarding this idea, the cytotoxic profiles we assessed demonstrated that both double-positive populations were presented in all three subsets, but statistically increased in Tc1 from WT animals, matching previous described concepts over Tc1 cytotoxicity.

FasL is an important molecule that controls survival of activated lymphocytes. In addition, FasL is an effector molecule of $CD4^+$ and $CD8^+$ T cells. Our findings revealed that all three $CD8^+$ T subsets from WT animals expressed similarly high percentage $FasL^+$ cells. This observation supports that our 3-day culture subsets demonstrated effector and cytolytic behavior of an activated $CD8^+$ T lymphocyte.

From the comparison between WT and *gld* mice, we could observe that, like WT, FasL-deficiency also generates effector activity after 3 days culture. However, it did not provide any significantly distinction in the production/expression of TNF-α, Granzyme B, Perforin, IL-4 and FasL, neither in the cytotoxic capacity of all three subsets. Although, it is worth mentioning that

the MFI means demonstrated visible differences, pointing out increased TNF-α, Granzyme B, and IL-4 in *gld* and Perforin in WT subsets. On the other hand, our findings uncovered that production of IFN-γ was significantly increased in Tc1 under FasL-deficiency condition. Nonetheless, further tests, increasing sample size could better investigate the means differences, also the prominent effect of FasL-deficiency on IFN-γ production.

6. Conclusions

We can sustain that our *in vitro* activation and Tc1/Tc2 polarization protocols have been positively working and present potential to be successfully applied to other mice lineages in future experiments. In overall, all three subsets presented effector feature and significant similarities during activation, also in the expression of effector molecules. Although, they demonstrated expected subset-specific behavior (by the expression of specific transcriptional factors, IFN-γ and others). Moreover, WT and *gld* animals statistically revealed very similar profiles of activation marks and effector molecules by FI-CD8 T, Tc0, Tc1 and Tc2 populations, with some punctual differences. Regarding those differences, we observed that FasL-deficiency might affect expression of CD62L and as consequence, influence the mechanisms shaping effector/memory-like behavior *in vitro*. Also, FasL reverse signaling could be related to the production and expression of IFN-γ in vitro, as some reports already described that IFN-γ production via IL-2 occur through other pathways, rather than through TCR signaling [108,123,124].

7. Future Perspectives

First of all, this work should also include the study of the AICD death mechanisms, testing same protocols and optimized conditions of activation and differentiation using *bim*$^{-/-}$ mouse strain. Not only that, but our polarization protocol should be extended to other effector CD8^{+} T subsets we described (Tc9, Tc17 and Tc22). Further tests, such as ELISA for cytokine analysis of culture

supernatant and MFC intracellular staining for Il-13 and IL-5, could help us understand the kinetics of TNF-α and IL-4 production. Moreover, we believe that experiments using cell sorting post-culture might be crucial to better understand the effectiveness of our polarization protocol. Future experiments should consider designs that apply bigger sample size (N), to improve statistical analysis. Furthermore, a completely metabolomic study would perfectly complement and support the understanding of *in vitro* activation and differentiation of $CD8^+$ T cells.

8. References

1. Travis, J. On the origin of the immune system. *Science (80-.).* (2009) doi:10.1126/science.324_580.
2. Iwasaki, A. & Medzhitov, R. Control of adaptive immunity by the innate immune system. *Nat. Immunol.* **16**, 343–353 (2015).
3. Gajewski, T. F., Schreiber, H. & Fu, Y. X. Innate and adaptive immune cells in the tumor microenvironment. *Nat. Immunol.* **14**, 1014–1022 (2013).
4. Basu, R. *et al.* Cytotoxic T Cells Use Mechanical Force to Potentiate Target Cell Killing. *Cell* **165**, 100–110 (2016).
5. World Health Organization. Cancer. https://www.who.int/en/news-room/fact-sheets/detail/cancer (2018).
6. Braciale, T. J. & Hahn, Y. S. Immunity to viruses. *Immunological Reviews* (2013) doi:10.1111/imr.12109.
7. Kucharski, A. J. *et al.* Early dynamics of transmission and control of COVID-19: a mathematical modelling study. *Lancet Infect. Dis.* **3099**, 1–7 (2020).
8. Liu, Y., Gayle, A. A., Wilder-Smith, A. & Rocklöv, J. The reproductive number of COVID-19 is higher compared to SARS coronavirus. *J. Travel Med.* **27**, 1–4 (2020).
9. Xu, Z. *et al.* Pathological findings of COVID-19 associated with acute respiratory distress syndrome. *Lancet Respir. Med.* **8**, 420–422 (2020).
10. Schwartz, R. H. T cell anergy. *Annu. Rev. Immunol.* **21**, 305–334 (2003).
11. Chapman, N. M., Boothby, M. R. & Chi, H. Metabolic coordination of T cell quiescence and activation. *Nat. Rev. Immunol.* **20**, 55–70 (2020).
12. Shin, H. & Iwasaki, A. Tissue-resident memory T cells. *Immunol. Rev.* **255**, 165–181 (2013).
13. Wherry, E. J., Barber, D. L., Kaech, S. M., Blattman, J. N. & Ahmed, R. Antigen-

independent memory CD8 T cells do not develop during chronic viral infection. *Proc. Natl. Acad. Sci. U. S. A.* **101**, 16004–16009 (2004).

14. Ruterbusch, M., Pruner, K. B., Shehata, L. & Pepper, M. In Vivo CD4+ T Cell Differentiation and Function: Revisiting the Th1/Th2 Paradigm. *Annu. Rev. Immunol.* **38**, 705–725 (2020).
15. Chen, Z. Y. *et al.* Decreased Expression of CD69 on T Cells in Tuberculosis Infection Resisters. *Front. Microbiol.* **11**, 1901 (2020).
16. Obar, J. J. & Lefrançois, L. Early events governing memory CD8 + T-cell differentiation. *Int. Immunol.* (2010) doi:10.1093/intimm/dxq053.
17. Spolski, R., Li, P. & Leonard, W. J. Biology and regulation of IL-2: from molecular mechanisms to human therapy. *Nat. Rev. Immunol.* **18**, 648–659 (2018).
18. Baaten, B. J. G. *et al.* CD44 Regulates Survival and Memory Development in Th1 Cells. *Immunity* **32**, 104–115 (2010).
19. Baaten, B. J. G., Tinoco, R., Chen, A. T. & Bradley, L. M. Regulation of antigen-experienced T cells: Lessons from the quintessential memory marker CD44. *Front. Immunol.* **3**, 23 (2012).
20. Klement, J. D. *et al.* An osteopontin/CD44 immune checkpoint controls CD8+ T cell activation and tumor immune evasion. *J. Clin. Invest.* **128**, 5549–5560 (2018).
21. Mielke, L. A. *et al.* TCF-1 limits the formation of Tc17 cells via repression of the MAF-RORγt axis. *J. Exp. Med.* **216**, 1682–1699 (2019).
22. Kaech, S. M. & Cui, W. Transcriptional control of effector and memory CD8+ T cell differentiation. *Nat. Rev. Immunol.* **12**, 749–761 (2012).
23. Backer, R. A. *et al.* A central role for Notch in effector CD8 + T cell differentiation. *Nat. Immunol.* **15**, 1143–1151 (2014).
24. Mittrücker, H. W., Visekruna, A. & Huber, M. Heterogeneity in the Differentiation and Function of CD8+ T Cells. *Arch. Immunol. Ther. Exp. (Warsz).* **62**, 449–458 (2014).

25. Yu, D. & Ye, L. A Portrait of CXCR5+ Follicular Cytotoxic CD8+ T cells. *Trends in Immunology* vol. 39 965–979 (2018).

26. St. Paul, M. & Ohashi, P. S. The Roles of CD8+ T Cell Subsets in Antitumor Immunity. *Trends in Cell Biology* vol. 30 695–704 (2020).

27. Li, J. *et al.* PD-1/SHP-2 inhibits Tc1/Th1 phenotypic responses and the activation of t cells in the tumor microenvironment. *Cancer Res.* **75**, 508–518 (2015).

28. Liu, J. *et al.* Type 1 Cytotoxic T Cells Increase in Placenta after Intrauterine Inflammation. *Front. Immunol.* **12**, 3670 (2021).

29. Annunziato, F., Romagnani, C. & Romagnani, S. The 3 major types of innate and adaptive cell-mediated effector immunity. *J. Allergy Clin. Immunol.* **135**, 626–635 (2015).

30. Voskoboinik, I., Whisstock, J. C. & Trapani, J. A. Perforin and granzymes: function, dysfunction and human pathology. *Nat. Rev. Immunol. 2015 156* **15**, 388–400 (2015).

31. Loo Yau, H. *et al.* DNA hypomethylating agents increase activation and cytolytic activity of CD8+ T cells. *Mol. Cell* **81**, 1469-1483.e8 (2021).

32. Balasubramani, A. *et al.* Modular utilization of distal cis-regulatory elements controls Ifng gene expression in T cells activated by distinct stimuli. *Immunity* **33**, 35–47 (2010).

33. Grange, M. *et al.* Active STAT5 Regulates T-bet and Eomesodermin Expression in CD8 T Cells and Imprints a T-bet–Dependent Tc1 Program with Repressed IL-6/TGF-β1 Signaling. *J. Immunol.* **191**, 3712–3724 (2013).

34. Paul, M. S. *et al.* IL6 induces an IL22+ CD8+ T-cell subset with potent antitumor function. *Cancer Immunol. Res.* **8**, 321–333 (2020).

35. Fahrner, J.-E. *et al.* The polarity and specificity of antiviral T lymphocyte responses determine susceptibility to SARS-CoV-2 infection in cancer patients and healthy individuals. *Cancer Discov.* (2022) doi:10.1158/2159-8290.CD-21-1441/681552/THE-POLARITY-AND-SPECIFICITY-OF-ANTIVIRAL-T.

36. Zeng, Q., Zhou, Y. & Schwarz, H. CD137L-DCs, Potent Immune-Stimulators—History,

Characteristics, and Perspectives. *Front. Immunol.* **10**, 2216 (2019).

37. Hayashi, K. *et al.* Tipping the immunostimulatory and inhibitory DAMP balance to harness immunogenic cell death. *Nat. Commun. 2020 111* **11**, 1–13 (2020).
38. Casalegno Garduño, R. & Däbritz, J. New Insights on CD8+ T Cells in Inflammatory Bowel Disease and Therapeutic Approaches. *Front. Immunol.* **12**, 4100 (2021).
39. Noble, A. *et al.* Deficient Resident Memory T Cell and CD8 T Cell Response to Commensals in Inflammatory Bowel Disease. *J. Crohn's Colitis* **14**, 525–537 (2020).
40. Rothe, K. *et al.* PIR-B expressing CD8+ T cells exhibit features of Tc1 and Tc17 in SKG mice. *Rheumatology* **58**, 2325–2329 (2019).
41. Iezzi, G. *et al.* Type 2 Cytotoxic T Lymphocytes Modulate the Activity of Dendritic Cells Toward Type 2 Immune Responses. *J. Immunol.* **177**, 2131–2137 (2006).
42. Kienzle, N., Buttigieg, K., Groves, P., Kawula, T. & Kelso, A. A Clonal Culture System Demonstrates That IL-4 Induces a Subpopulation of Noncytolytic T Cells with Low CD8, Perforin, and Granzyme Expression. *J. Immunol.* **168**, 1672–1681 (2002).
43. Kienzle, N. *et al.* Progressive Differentiation and Commitment of CD8+ T Cells to a Poorly Cytolytic CD8low Phenotype in the Presence of IL-4. *J. Immunol.* **174**, 2021–2029 (2005).
44. Harland, K. L. *et al.* Epigenetic plasticity of Cd8a locus during CD8+ T-cell development and effector differentiation and reprogramming. *Nat. Commun. 2014 51* **5**, 1–13 (2014).
45. Fox, A., Harland, K. L., Kedzierska, K. & Kelso, A. Exposure of human CD8+ T cells to type-2 cytokines impairs division and differentiation and induces limited polarization. *Front. Immunol.* **9**, 1141 (2018).
46. Ning, F. *et al.* Hypoxia enhances CD8+ TC2 cell–dependent airway hyperresponsiveness and inflammation through hypoxia-inducible factor 1α. *J. Allergy Clin. Immunol.* **143**, 2026-2037.e7 (2019).
47. Jia, Y. *et al.* Steroidogenic enzyme Cyp11a1 regulates Type 2 CD8+ T cell skewing in allergic lung disease. *Proc. Natl. Acad. Sci. U. S. A.* **110**, 8152–8157 (2013).

48. Schedel, M. *et al.* 1,25D3 prevents CD8+Tc2 skewing and asthma development through VDR binding changes to the Cyp11a1 promoter. *Nat. Commun. 2016 71* **7**, 1–11 (2016).

49. Ma, X. *et al.* Cholesterol negatively regulates IL-9-producing CD8+ T cell differentiation and antitumor activity. *J. Exp. Med.* **215**, 1555–1569 (2018).

50. Lu, Y., Wang, Q. & Yi, Q. Anticancer Tc9 cells: Long-lived tumor-killing T cells for adoptive therapy. *https://doi.org/10.4161/onci.28542* **3**, e28542 (2014).

51. Lu, Y. *et al.* Tumor-specific IL-9-producing CD8+ Tc9 cells are superior effector than type-I cytotoxic Tc1 cells for adoptive immunotherapy of cancers. *Proc. Natl. Acad. Sci. U. S. A.* **111**, 2265–2270 (2014).

52. Xiao, L. *et al.* IL-9/STAT3/fatty acid oxidation-mediated lipid peroxidation contributes to Tc9 cell longevity and enhanced antitumor activity. *J. Clin. Invest.* (2022) doi:10.1172/JCI153247.

53. Visekruna, A. *et al.* Tc9 cells, a new subset of CD8+ T cells, support Th2-mediated airway inflammation. *Eur. J. Immunol.* **43**, 606–618 (2013).

54. Dardalhon, V. *et al.* IL-4 inhibits TGF-β-induced Foxp3+ T cells and, together with TGF-β, generates IL-9+ IL-10+ Foxp3− effector T cells. *Nat. Immunol. 2008 912* **9**, 1347–1355 (2008).

55. Huber, M. & Lohoff, M. IRF4 at the crossroads of effector T-cell fate decision. *Eur. J. Immunol.* **44**, 1886–1895 (2014).

56. Jiang, H., Fu, D., Bidgoli, A. & Paczesny, S. T Cell Subsets in Graft Versus Host Disease and Graft Versus Tumor. *Front. Immunol.* **12**, 4031 (2021).

57. Huber, M. *et al.* IL-17A secretion by CD8+ T cells supports Th17-mediated autoimmune encephalomyelitis. *J. Clin. Invest.* **123**, 247–260 (2013).

58. Lückel, C. *et al.* IL-17+ CD8+ T cell suppression by dimethyl fumarate associates with clinical response in multiple sclerosis. *Nat. Commun. 2019 101* **10**, 1–15 (2019).

59. Lückel, C., Picard, F. S. R. & Huber, M. Tc17 biology and function: Novel concepts. *Eur.*

J. Immunol. **50**, 1257–1267 (2020).

60. Saxena, A. *et al.* Tc17 CD8+ T Cells Potentiate Th1-Mediated Autoimmune Diabetes in a Mouse Model. *J. Immunol.* **189**, 3140–3149 (2012).

61. Yen, H.-R. *et al.* Tc17 CD8 T Cells: Functional Plasticity and Subset Diversity. *J. Immunol.* **183**, 7161–7168 (2009).

62. Sales, M. C. *et al.* Selective serotonin reuptake inhibitor attenuates the hyperresponsiveness of TLR2+ and TLR4+ Th17/Tc17-like cells in multiple sclerosis patients with major depression. *Immunology* **162**, 290–305 (2021).

63. Nanjappa, S. G. *et al.* Antifungal Tc17 cells are durable and stable, persisting as long-lasting vaccine memory without plasticity towards IFNγ cells. *PLOS Pathog.* **13**, e1006356 (2017).

64. Ohkuri, T., Kosaka, A., Ikeura, M., Salazar, A. M. & Okada, H. IFN-γ- and IL-17-producing CD8 + T (Tc17-1) cells in combination with poly-ICLC and peptide vaccine exhibit antiglioma activity. *J. Immunother. cancer* **9**, (2021).

65. Kim, B. S. *et al.* Type 17 immunity promotes the exhaustion of CD8+ T cells in cancer. *J. Immunother. Cancer* **9**, e002603 (2021).

66. Liu, J. *et al.* Single-cell RNA sequencing of psoriatic skin identifies pathogenic Tc17 cell subsets and reveals distinctions between CD8+ T cells in autoimmunity and cancer. *J. Allergy Clin. Immunol.* **147**, 2370–2380 (2021).

67. Oliveira, L. M. S. *et al.* Increased frequency of circulating Tc22/Th22 cells and polyfunctional CD38− T cells in HIV-exposed uninfected subjects. *Sci. Reports 2015 51* **5**, 1–9 (2015).

68. Song, Q. *et al.* IL-22-dependent dysbiosis and mononuclear phagocyte depletion contribute to steroid-resistant gut graft-versus-host disease in mice. *Nat. Commun. 2021 121* **12**, 1–19 (2021).

69. St. Paul, M. *et al.* Coenzyme A fuels T cell anti-tumor immunity. *Cell Metab.* **33**, 2415-

2427.e6 (2021).

70. Bourgin, M., Kepp, O. & Kroemer, G. Immunostimulatory effects of vitamin B5 improve anticancer immunotherapy. *https://doi.org/10.1080/2162402X.2022.2031500* **11**, (2022).

71. Laidlaw, B. J. *et al.* Production of IL-10 by CD4+ regulatory T cells during the resolution of infection promotes the maturation of memory CD8+ T cells. *Nat. Immunol.* **16**, 871–879 (2015).

72. Russ, B. E. *et al.* Distinct epigenetic signatures delineate transcriptional programs during virus-specific CD8+ T cell differentiation. *Immunity* **41**, 853–865 (2014).

73. Arakaki, R., Yamada, A., Kudo, Y., Hayashi, Y. & Ishimaru, N. Mechanism of activation-induced cell death of T cells and regulation of FasL expression. *Crit. Rev. Immunol.* **34**, 301–314 (2014).

74. Brenner, D., Krammer, P. H. & Arnold, R. Concepts of activated T cell death. *Crit. Rev. Oncol. Hematol.* **66**, 52–64 (2008).

75. Czabotar, P. E., Lessene, G., Strasser, A. & Adams, J. M. Control of apoptosis by the BCL-2 protein family: implications for physiology and therapy. *Nat. Rev. Mol. Cell Biol. 2014 151* **15**, 49–63 (2013).

76. Pistritto, G., Trisciuoglio, D., Ceci, C., Alessia Garufi & D'Orazi, G. Apoptosis as anticancer mechanism: Function and dysfunction of its modulators and targeted therapeutic strategies. *Aging (Albany. NY).* **8**, 603–619 (2016).

77. Wang, K. Molecular mechanisms of hepatic apoptosis. *Cell Death Dis.* **5**, (2014).

78. Zhang, N., Hartig, H., Dzhagalov, I., Draper, D. & He, Y. W. The role of apoptosis in the development and function of T lymphocytes. *Cell Res. 2005 1510* **15**, 749–769 (2005).

79. Chen & Zander. T-cell death following immune activation is mediated by mitochondria-localized SARM. *Cell Death Differ.* **20**, 478–489 (2013).

80. Zhan, Y., Carrington, E. M., Zhang, Y., Heinzel, S. & Lew, A. M. Life and death of activated T cells: How are they different from naïve T Cells? *Front. Immunol.* **8**, 1–9

(2017).

81. Martin, M. D. & Badovinac, V. P. Defining memory CD8 T cell. *Frontiers in Immunology* vol. 9 (2018).

82. Jiang, X. *et al.* Skin infection generates non-migratory memory CD8 + T RM cells providing global skin immunity. *Nature* **483**, 227–231 (2012).

83. Steinert, E. M. *et al.* Quantifying Memory CD8 T Cells Reveals Regionalization of Immunosurveillance. *Cell* **161**, 737–749 (2015).

84. Kok, L., Masopust, D. & Schumacher, T. N. The precursors of CD8+ tissue resident memory T cells: from lymphoid organs to infected tissues. *Nat. Rev. Immunol. 22, 225* **22**, 283–293 (2022).

85. Martin, M. D. & Badovinac, V. P. Defining memory CD8 T cell. *Front. Immunol.* **9**, 1–10 (2018).

86. Gerlach, C. *et al.* The Chemokine Receptor CX3CR1 Defines Three Antigen-Experienced CD8 T Cell Subsets with Distinct Roles in Immune Surveillance and Homeostasis. *Immunity* **45**, 1270–1284 (2016).

87. Pais Ferreira, D. *et al.* Central memory CD8+ T cells derive from stem-like Tcf7hi effector cells in the absence of cytotoxic differentiation. *Immunity* **53**, 985-1000.e11 (2020).

88. Youngblood, B. *et al.* Effector CD8 T cells dedifferentiate into long-lived memory cells. *Nat. 2017 5527685* **552**, 404–409 (2017).

89. Kakaradov, B. *et al.* Early transcriptional and epigenetic regulation of CD8 + T cell differentiation revealed by single-cell RNA sequencing. *Nat. Immunol.* **18**, 422–432 (2017).

90. Anuradha, R. *et al.* Modulation of CD4+ and CD8+ T cell function and cytokine responses in Strongyloides stercoralis infection by interleukin-27 (IL-27) and IL-37. *Infect. Immun.* **85**, (2017).

91. Pace, L. *et al.* The epigenetic control of stemness in CD8+ T cell fate commitment.

Science (80-.). **359**, 177–186 (2018).

92. Verdon, D. J., Mulazzani, M. & Jenkins, M. R. Cellular and Molecular Mechanisms of CD8+ T Cell Differentiation, Dysfunction and Exhaustion. *Int. J. Mol. Sci. 2020, Vol. 21, Page 7357* **21**, 7357 (2020).
93. Herndler-Brandstetter, D. *et al.* KLRG1+ Effector CD8+ T Cells Lose KLRG1, Differentiate into All Memory T Cell Lineages, and Convey Enhanced Protective Immunity. *Immunity* **48**, 716-729.e8 (2018).
94. Corgnac, S. *et al.* CD103 + CD8 + T RM Cells Accumulate in Tumors of Anti-PD-1-Responder Lung Cancer Patients and Are Tumor-Reactive Lymphocytes Enriched with Tc17. *Cell reports. Med.* **1**, (2020).
95. Behr, F. M. *et al.* Tissue-resident memory CD8+ T cells shape local and systemic secondary T cell responses. *Nat. Immunol. 2020 219* **21**, 1070–1081 (2020).
96. Topham, D. J. & Reilly, E. C. Tissue-resident memory CD8+ T cells: From phenotype to function. *Front. Immunol.* **9**, 515 (2018).
97. Böttcher, J. P. *et al.* Functional classification of memory CD8(+) T cells by CX3CR1 expression. *Nat. Commun.* **6**, (2015).
98. Ferenczi, K., Burack, L., Pope, M., Krueger, J. G. & Austin, L. M. CD69, HLA-DR and the IL-2R Identify Persistently Activated T Cells in Psoriasis Vulgaris Lesional Skin: Blood and Skin Comparisons by Flow Cytometry. *J. Autoimmun.* **14**, 63–78 (2000).
99. Naghizadeh, M. *et al.* Kinetics of activation marker expression after in vitro polyclonal stimulation of chicken peripheral T cells. *Cytom. Part A* **101**, 45–56 (2022).
100. Huss, D. J. *et al.* Anti-CD25 monoclonal antibody Fc variants differentially impact regulatory T cells and immune homeostasis. *Immunology* **148**, 276–286 (2016).
101. Cibrián, D. & Sánchez-Madrid, F. CD69: from activation marker to metabolic gatekeeper. *Eur. J. Immunol.* **47**, 946–953 (2017).
102. González-Amaro, R., Cortés, J. R., Sánchez-Madrid, F. & Martín, P. Is CD69 an effective

brake to control inflammatory diseases? *Trends Mol. Med.* **19**, 625–632 (2013).

103. Koda, Y. *et al.* CD8+ tissue-resident memory T cells promote liver fibrosis resolution by inducing apoptosis of hepatic stellate cells. *Nat. Commun. 2021 121* **12**, 1–15 (2021).

104. Ivetic, A., Green, H. L. H. & Hart, S. J. L-selectin: A major regulator of leukocyte adhesion, migration and signaling. *Front. Immunol.* **10**, 1068 (2019).

105. Hochheiser, K. *et al.* Ptpn2 and KLRG1 regulate the generation and function of tissue-resident memory CD8+ T cells in skin. *J. Exp. Med.* **218**, (2021).

106. Nakajima, Y., Chamoto, K., Oura, T. & Honjo, T. Critical role of the CD44lowCD62Llow CD8+ T cell subset in restoring antitumor immunity in aged mice. *Proc. Natl. Acad. Sci. U. S. A.* **118**, e2103730118 (2021).

107. Sahu, R. *et al.* A nanovaccine formulation of Chlamydia recombinant MOMP encapsulated in PLGA 85:15 nanoparticles augments CD4+ effector (CD44high CD62Llow) and memory (CD44high CD62Lhigh) T-cells in immunized mice. *Nanomedicine Nanotechnology, Biol. Med.* **29**, 102257 (2020).

108. Rackov, G. *et al.* Mitochondrial reactive oxygen is critical for IL-12/IL-18-induced IFN-γ production by CD4+ T cells and is regulated by Fas/FasL signaling. *Cell Death Dis. 2022 136* **13**, 1–14 (2022).

109. Tarzi, R. M. *et al.* Mice with defective Fas ligand are protected from crescentic glomerulonephritis. *Kidney Int.* **81**, 170–178 (2012).

110. Takahashi, T. *et al.* Generalized lymphoproliferative disease in mice, caused by a point mutation in the fas ligand. *Cell* **76**, 969–976 (1994).

111. Koshkina, N., Yang, Y. & Kleinerman, E. S. The Fas/FasL signaling pathway: Its role in the metastatic process and as a target for treating osteosarcoma lung metastases. *Adv. Exp. Med. Biol.* **1258**, 177–187 (2020).

112. Krzyzowska, M., Kowalczyk, A., Skulska, K., Thörn, K. & Eriksson, K. Fas/FasL Contributes to HSV-1 Brain Infection and Neuroinflammation. *Front. Immunol.* **12**, 3555

(2021).

113. Suenaga, F. *et al.* Loss of Lymph Node Fibroblastic Reticular Cells and High Endothelial Cells Is Associated with Humoral Immunodeficiency in Mouse Graft-versus-Host Disease. *J. Immunol.* **194**, 398–406 (2015).

114. Rodriguez, A. *et al.* Requirement of bic/microRNA-155 for normal immune function. *Science (80-.).* **316**, 608–611 (2007).

115. Dobrzanski, M. J., Reome, J. B., Hollenbaugh, J. A., Hylind, J. C. & Dutton, R. W. Effector Cell-Derived Lymphotoxin α and Fas Ligand, but not Perforin, Promote Tc1 and Tc2 Effector Cell-Mediated Tumor Therapy in Established Pulmonary Metastases. *Cancer Res.* **64**, 406–414 (2004).

116. Brehm, M. A. *et al.* Rapid quantification of naive alloreactive T cells by TNF-α production and correlation with allograft rejection in mice. *Blood* **109**, 819–826 (2007).

117. Brehm, M. A., Daniels, K. A. & Welsh, R. M. Rapid Production of TNF-α following TCR Engagement of Naive CD8 T Cells. *J. Immunol.* **175**, 5043–5049 (2005).

118. Golstein, P. & Griffiths, G. M. An early history of T cell-mediated cytotoxicity. *Nat. Rev. Immunol. 2018 188* **18**, 527–535 (2018).

119. Seder, R. A., Darrah, P. A. & Roederer, M. T-cell quality in memory and protection: implications for vaccine design. *Nat. Rev. Immunol. 2008 84* **8**, 247–258 (2008).

120. Rodrigues, L. S. *et al.* Multifunctional, TNF-α and IFN-γ-Secreting CD4 and CD8 T Cells and CD8High T Cells Are Associated With the Cure of Human Visceral Leishmaniasis. *Front. Immunol.* **12**, 4433 (2021).

121. Wang, Y., Radfar, S. & Khong, H. T. Activated CD4+T cells enhance radiation effect through the cooperation of interferon-γ and TNF-α. *BMC Cancer* **10**, 1–13 (2010).

122. Glaser, F. *et al.* Liver infiltrating T cells regulate bile acid metabolism in experimental cholangitis. *J. Hepatol.* **71**, 783–792 (2019).

123. Papadakis, K. A. *et al.* Dominant Role for TL1A/DR3 Pathway in IL-12 plus IL-18-Induced

IFN-γ Production by Peripheral Blood and Mucosal CCR9+ T Lymphocytes. *J. Immunol.* **174**, 4985–4990 (2005).

124. Balasubramani, A. *et al.* Modular utilization of distal cis-regulatory elements controls Ifng gene expression in T cells activated by distinct stimuli. *Immunity* **33**, 35–47 (2010).